D_2 receptors, as determined on the seventh day following treatment cessation. As regards the Bmax value (ie, density) of the D_2 receptors, the HAL-HAL group showed significantly higher Bmax values than either the VEH-VEH or the HAL-ARI group (ie, averaged 240% and 97% higher, respectively), whereas there was no significant difference between the HAL-ARI group and the VEH-VEH group ($P < .05$; figure 5B). Furthermore, the Bmax value in the HAL-ARI group was significantly lower (ie, an average of 49% lower) than that of the HAL-HAL group, whereas no significant differences were observed between the HAL-HAL and the HAL-VEH groups ($P < .05$; figure 5B). Consequently, the rank order of the D_2 density was HAL-HAL > HAL-VEH > HAL-ARI > VEH-VEH, which was the same ranking as seen in the locomotor study. On the other hand, as regards the Kd values (ie, affinity) of the D_2 receptors, there were no significant differences among the 4 groups ($P < .05$; figure 5A).

Discussion

In the present study, we investigated the effects of chronic treatment with minipump-administered HAL, ARI, or VEH on the sensitivity of rats to dopamine, as measured by the locomotor response to MAP and the density of striatal D_2 receptors on the seventh day following treatment cessation. Chronic treatment with HAL significantly increased the rats' locomotor response and the striatal D_2 density compared with the values observed after chronic treatment with either VEH or ARI. Moreover, there were no significant differences between the VEH and ARI groups in terms of locomotor response or D_2 density. We also investigated the effects of chronic treatment with HAL, ARI, or VEH following chronic treatment with HAL or VEH on locomotor response and D_2 receptor density. The ANOVA analysis indicated the same rank ordering of groups in terms of either locomotor response or D_2 receptor density, ie, HAL-HAL > HAL-VEH > HAL-ARI > VEH-VEH. These results indicate that chronic treatment with HAL induces dopamine supersensitivity, which is retained for an extended period of time, and is exacerbated by additional HAL treatment. In contrast, chronic treatment with ARI does not induce dopamine supersensitivity, and it reduces the supersensitivity induced by the preceding chronic treatment with HAL.

In order to investigate the effects of chronic antipsychotic treatment, we implanted rats with an Alzet osmotic minipump, which enabled the continuous administration of drugs at a constant rate. It has been reported that a protocol of either single or twice-daily injection, such as that adopted in most previous studies, may not suffice as a preclinical model because the half-life of antipsychotic agents is, on average, 4 to 6 times faster in rodents than in humans.[20] For instance, the half-life of HAL is 1.5 h in rodents vs 12-36 h in humans[21,22] and that of ARI is 1.9-2.2 h in rodents vs 47-68 h in humans.[23,24]

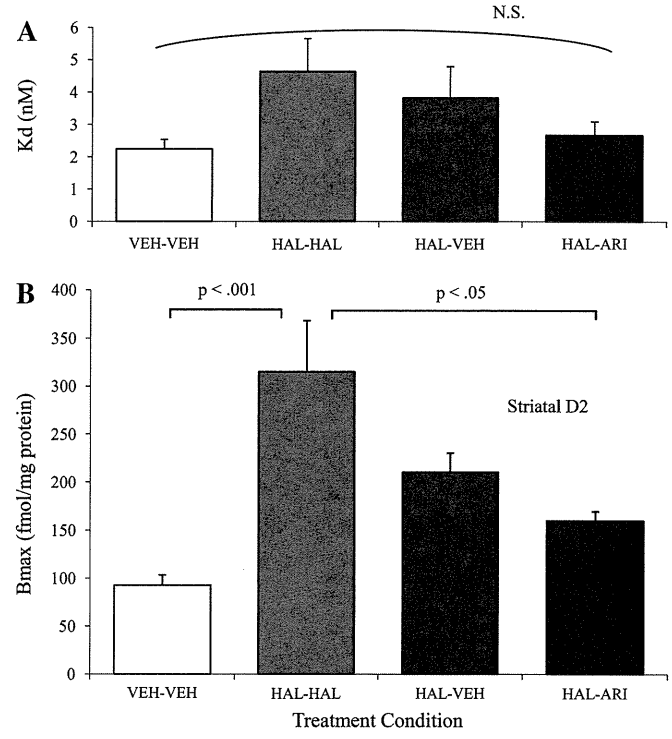

Fig. 5. The effects of chronic treatment with haloperidol (0.75 mg/kg/d, HAL-HAL), aripiprazole (1.5 mg/kg/d, HAL-ARI), or vehicle (HAL-VEH), preceded by chronic treatment with HAL (0.75 mg/kg/d) or VEH (VEH-VEH), on Kd (A) and Bmax (B) of striatal D_2 receptors. Either HAL or VEH was administered via an implanted minipump for 14 days and then the minipump was exchanged for a second minipump, by which drugs were administered for an additional 14 days. The animals were decapitated on the seventh day following the cessation of the entire 28-day treatment period. In (A), there was no significant difference in the Kd value of any of the groups (one-way ANOVA; $F_3 = 2.13$; $P = .150$). In (B), the Bmax value of the HAL-HAL group was significantly higher than that of either the VEH-VEH group or the HAL-ARI group (one-way ANOVA with Bonferroni's tests; $F_3 = 10.33$; $P < .001$ [HAL-HAL vs VEH-VEH]; $P < .05$ [HAL-HAL vs HAL-ARI]). There was also a significant difference between Bmax values among the HAL-HAL, HAL-VEH, and HAL-ARI groups (one-way ANOVA; $F_2 = 5.72$; $P < .05$). In the post hoc analyses on the Bmax value, the HAL-ARI group had a significantly lower value than that of the HAL-HAL group, whereas there was no significant difference between the Bmax values of the HAL-HAL group and the HAL-VEH group (Bonferroni's tests; $P < .05$ [HAL-HAL vs HAL-ARI]; $P = .156$ [HAL-HAL vs HAL-VEH]). The rank ordering of groups in terms of D_2 density was HAL-HAL > HAL-VEH > HAL-ARI > VEH-VEH. $N = 4$ in each group. Error bars indicate the SEM.

Kapur et al[20] suggested that only when doses 5 times higher than the optimal single injection were administered by minipump were clinically comparable D_2 occupancies obtained. Thus, the present study protocol serves as an appropriate animal model of chronic antipsychotic treatment.

In the present study, we found that chronic treatment with ARI did not induce behavioral supersensitivity, which result may have been due to the maintenance of

stable striatal D_2 receptor density, in accord with the findings of a previous study.[25] Interestingly, we also observed that chronic treatment with ARI reduced the dopamine supersensitivity previously induced by chronic HAL treatment, as determined based on both behavioral testing and D_2 receptor density. In other words, ARI left baseline dopamine sensitivity intact in drug-naive rats, while it reduced sensitivity in rats that had already developed supersensitivity. Although it was already known that chronic exposure to agonists often induces desensitization that correlates with a decrease in the number of targeted receptors,[26] ARI did not induce desensitization in drug-naive rats. One explanation for these results could be related to compensatory systems of dopamine neurotransmission. Although it is still controversial whether ARI is a D_2 receptor partial agonist,[27–29] ARI is thought to possess some dopamine agonistic activity.[30] Hence, in drug-naive rats, ARI allows for natural dopaminergic neurotransmission, and such compensatory functioning may not be involved. On the other hand, in supersensitive rats, ARI yields excessive dopaminergic neurotransmission due to increased D_2 receptor density, and thus compensatory systems may be induced, which in turn would reduce D_2 receptor density, as suggested in the present study. In other words, ARI may stabilize sensitivity to dopamine by regulating compensatory systems of dopamine neurotransmission.

Chronic treatment with D_2-antagonistic antipsychotics in some cases induces dopamine supersensitivity, which may cause supersensitivity psychosis and may ultimately be related to treatment-resistant schizophrenia. In fact, it has been estimated that more than half of treatment-resistant schizophrenia cases may be related to supersensitivity psychosis.[31] The results of the present study suggest that chronic ARI administration may reduce the risk of supersensitivity psychosis, which might be related to a lower rate of rehospitalization. Although a transient worsening of psychosis can appear in certain supersensitized patients due to relatively excessive agonistic effects,[32] ARI may be a helpful agent for patients with treatment-resistant schizophrenia by reducing excessive sensitivity to dopamine.

Acknowledgments

The authors would like to thank Prof Yukihiko Shirayama (Department of Psychiatry, Teikyo University Chiba Medical Center) for his encouragement during the early stages of the study and for his technical support with the rat experiments, Dr Jin Wu (Chiba University for Forensic Mental Health) for her technical advice on the radioligand binding assays, and Mrs Yuko Fujita (Chiba University for Forensic Mental Health) for her advice regarding the general treatment of laboratory rats. The Authors have declared that there are no conflicts of interest in relation to the subject of this study.

Funding

Funding to pay the Open Access publication charges for this article was provided by the Department of Psychiatry, Chiba University Graduate School of Medicine, Chiba, Japan.

References

1. Snyder SH. Dopamine receptors, neuroleptics, and schizophrenia. *Am J Psychiatry*. 1981;138:460–464.
2. Kane JM. Treatment strategies to prevent relapse and encourage remission. *J Clin Psychiatry*. 2007;68(suppl 14):27–30.
3. Weiden P, Rapkin B, Zygmunt A, Mott T, Goldman D, Frances A. Postdischarge medication compliance of inpatients converted from an oral to a depot neuroleptic regimen. *Psychiatr Serv*. 1995;46:1049–1054.
4. Carpenter WT, McGlashan TH, Strauss JS. The treatment of acute schizophrenia without drugs: an investigation of some current assumptions. *Am J Psychiatry*. 1977;134(1):14–20.
5. Davis KL, Rosenberg GS. Is there a limbic system equivalent of tardive dyskinesia? *Biol Psychiatry*. 1979;14:699–703.
6. Chouinard G, Jones BD, Annable L. Neuroleptic-induced supersensitivity psychosis. *Am J Psychiatry*. 1978;135:1409–1410.
7. Chouinard G, Jones BD. Neuroleptic-induced supersensitivity psychosis: clinical and pharmacologic characteristics. *Am J Psychiatry*. 1980;137(1):16–21.
8. Chouinard G, Creese I, Boisvert D, Annable L, Bradwejn J, Jones B. High neuroleptic plasma levels in patients manifesting supersensitivity psychosis. *Biol Psychiatry*. 1982;17:849–852.
9. Chouinard G. Severe cases of neuroleptic-induced supersensitivity psychosis. Diagnostic criteria for the disorder and its treatment. *Schizophr Res*. 1991;5(1):21–33.
10. Kirkpatrick B, Alphs L, Buchanan RW. The concept of supersensitivity psychosis. *J Nerv Ment Dis*. 1992;180:265–270.
11. Gorwood P. Meeting everyday challenges: antipsychotic therapy in the real world. *Eur Neuropsychopharmacol*. 2006;16(suppl 3):S156–S162.
12. Murugaiah K, Theodorou A, Mann S, Clow A, Jenner P, Marsden CD. Chronic continuous administration of neuroleptic drugs alters cerebral dopamine receptors and increases spontaneous dopaminergic action in the striatum. *Nature*. 1982;296:570–572.
13. Sasaki H, Hashimoto K, Inada T, Fukui S, Iyo M. Suppression of oro-facial movements by rolipram, a cAMP phosphodiesterase inhibitor, in rats chronically treated with haloperidol. *Eur J Pharmacol*. 1995;282(1–3):71–76.
14. Sasaki H, Hashimoto K, Maeda Y, et al. Rolipram, a selective c-AMP phosphodiesterase inhibitor suppresses oro-facial dyskinetic movements in rats. *Life Sci*. 1995;56:PL443–P447.
15. Seeman P, Schwarz J, Chen JF, et al. Psychosis pathways converge via D2high dopamine receptors. *Synapse*. 2006;60:319–346.
16. Samaha AN, Seeman P, Stewart J, Rajabi H, Kapur S. "Breakthrough" dopamine supersensitivity during ongoing antipsychotic treatment leads to treatment failure over time. *J Neurosci*. 2007;27:2979–2986.

17. Ohmori T, Miura S, Yamashita I, et al. Late phase II study of aripiprazole for schizophrenia. *Jpn J Clin Psychopharmacol.* 2006;9:271–293.
18. Asakura W, Matsumoto K, Ohta H, Watanabe H. REM sleep deprivation decreases apomorphine-induced stimulation of locomotor activity but not stereotyped behavior in mice. *Gen Pharmacol.* 1992;23:337–341.
19. Huang N, Ase AR, Hebert C, van Gelder NM, Reader TA. Effects of chronic neuroleptic treatments on dopamine D1 and D2 receptors: homogenate binding and autoradiographic studies. *Neurochem Int.* 1997;30:277–290.
20. Kapur S, VanderSpek SC, Brownlee BA, Nobrega JN. Antipsychotic dosing in preclinical models is often unrepresentative of the clinical condition: a suggested solution based on in vivo occupancy. *J Pharmacol Exp Ther.* 2003;305:625–631.
21. Cheng YF, Paalzow LK. Linear pharmacokinetics of haloperidol in the rat. *Biopharm Drug Dispos.* 1992;13(1):69–76.
22. Bezchlibnyk-Butler KZ, Jeffries JJ. *Clinical Handbook of Psychotropic Drugs.* Toronto, ON: Hogrefe & Huber Publishers; 1999.
23. Shimokawa Y, Akiyama H, Kashiyama E, Koga T, Miyamoto G. High performance liquid chromatographic methods for the determination of aripiprazole with ultraviolet detection in rat plasma and brain: application to the pharmacokinetic study. *J Chromatogr B Analyt Technol Biomed Life Sci.* 2005;821(1):8–14.
24. Mauri MC, Volonteri LS, Colasanti A, Fiorentini A, De Gaspari IF, Bareggi SR. Clinical pharmacokinetics of atypical antipsychotics: a critical review of the relationship between plasma concentrations and clinical response. *Clin Pharmacokinet.* 2007;46:359–388.
25. Inoue A, Miki S, Seto M, et al. Aripiprazole, a novel antipsychotic drug, inhibits quinpirole-evoked GTPase activity but does not up-regulate dopamine D2 receptor following repeated treatment in the rat striatum. *Eur J Pharmacol.* 1997;321(1):105–111.
26. Tsai SJ. Dopamine receptor downregulation: an alternative strategy for schizophrenia treatment. *Med Hypotheses.* 2004;63:1047–1050.
27. Lawler CP, Prioleau C, Lewis MM, et al. Interactions of the novel antipsychotic aripiprazole (OPC-14597) with dopamine and serotonin receptor subtypes. *Neuropsychopharmacology.* 1999;20:612–627.
28. Shapiro DA, Renock S, Arrington E, et al. Aripiprazole, a novel atypical antipsychotic drug with a unique and robust pharmacology. *Neuropsychopharmacology.* 2003;28:1400–1411.
29. Urban JD, Vargas GA, von Zastrow M, Mailman RB. Aripiprazole has functionally selective actions at dopamine D2 receptor-mediated signaling pathways. *Neuropsychopharmacology.* 2007;32(1):67–77.
30. Burris KD, Molski TF, Xu C, et al. Aripiprazole, a novel antipsychotic, is a high-affinity partial agonist at human dopamine D2 receptors. *J Pharmacol Exp Ther.* 2002;302:381–389.
31. Chouinard G, Chouinard VA. Atypical antipsychotics: CATIE study, drug-induced movement disorder and resulting iatrogenic psychiatric-like symptoms, supersensitivity rebound psychosis and withdrawal discontinuation syndromes. *Psychother Psychosom.* 2008;77(2):69–77.
32. Di Lorenzo R, Amoretti A, Forghieri M, Fiorini F, Genedani S, Rigatelli M. Aripiprazole: effectiveness and safety under naturalistic conditions. *Exp Clin Psychopharmacol.* 2007;15:569–575.

Psychopharmacology (2012) 222:37–45
DOI 10.1007/s00213-011-2619-3

ORIGINAL INVESTIGATION

Protective effects of the antioxidant sulforaphane on behavioral changes and neurotoxicity in mice after the administration of methamphetamine

Hongxian Chen · Jin Wu · Jichun Zhang · Yuko Fujita · Tamaki Ishima · Masaomi Iyo · Kenji Hashimoto

Received: 19 June 2011 / Accepted: 12 December 2011 / Published online: 27 December 2011

Abstract
Rationale Methamphetamine (METH) is a powerfully addictive stimulant associated with serious health conditions. Accumulating evidence suggests a role of oxidative stress in METH-induced behavioral abnormalities. Sulforaphane (SFN), found in cruciferous vegetables, is a potent antioxidant. It is of interest to determine whether SFN can attenuate behavioral and neuropathological changes associated with METH exposure.
Objectives This study was undertaken to examine the effects of SFN on behavioral changes and dopaminergic neurotoxicity in mice exposed to METH.
Methods The effects of SFN on acute hyperlocomotion and the development of behavioral sensitization induced by the administration of METH were examined. Levels of dopamine (DA) and its major metabolite 3,4-dihydroxyphenyl acetic acid (DOPAC) in the striatum were measured. In addition, DA transporter (DAT) immunoreactivity was also performed.
Results Pretreatment with SFN at 1, 3, and 10 mg/kg elicited a dose-dependent attenuation of acute hyperlocomotion in mice, after a single administration of METH (3 mg/kg). The development of behavioral sensitization after repeated administrations of METH (3 mg/kg/day, once daily for 5 days) was significantly reduced by pretreatment with SFN (10 mg/kg). In addition, the lowering of DA levels and DOPAC as well as DAT immunoreactivity in the striatum, usually seen after repeated administration of METH, was significantly attenuated by both pretreatment and the subsequent administration of SFN. Furthermore, SFN significantly reduced microglial activation in the striatum after repeated exposure to METH.
Conclusion It is therefore likely that SFN can be a useful drug for the treatment of signs associated with METH abuse in humans.

Keywords Sulforaphane · Dopamine · Methamphetamine · Microglia · Neurotoxicity · Sensitization

Abbreviations

METH	Methamphetamine
SFN	Sulforaphane
DA	Dopamine
DOPAC	3,4-Dihydroxyphenyl acetic acid
DAT	Dopamine transporter
PET	Positron emission tomography
Nrf2	NF-E2-related factor-2
ARE	Antioxidant responsive element
HPLC	High performance liquid chromatography

Electronic supplementary material The online version of this article (doi:10.1007/s00213-011-2619-3) contains supplementary material, which is available to authorized users.

H. Chen · J. Wu · J. Zhang · Y. Fujita · T. Ishima · K. Hashimoto (✉)
Division of Clinical Neuroscience,
Chiba University Center for Forensic Mental Health,
1-8-1 Inohana,
Chiba 260-8670, Japan
e-mail: hashimoto@faculty.chiba-u.jp

H. Chen
Mental Health Institute,
WHO Collaborating Center for Drug Abuse and Health,
Second Xiangya Hospital, Central South University,
Changsha, Hunan 410011, People's Republic of China

M. Iyo
Department of Psychiatry,
Chiba University Graduate School of Medicine,
Chiba 260-8670, Japan

Introduction

Abuse of methamphetamine (METH) is an extremely serious and growing global problem, affecting the USA and Asian countries such as Japan, South Korea, Thailand, Philippines, and China (National Institute on Drug Abuse 2002; Yamamoto 2004; Barr et al. 2006; Hashimoto 2007; United Nations Office on Drug Use and Crime (UNODC) 2008; Gonzales et al. 2010; Chen et al. 2010; Colfax et al. 2010). METH is a powerfully addictive stimulant associated with serious health conditions, including memory loss, aggression, psychotic signs, and brain damage (Ujike and Sato 2004; Hashimoto 2007; Chen et al. 2010). However, there is currently no pharmacological treatment for the wide range of signs associated with METH exposure (Hashimoto 2007; Chen et al. 2010).

Repeated administration of METH is known to induce dopaminergic neurotoxicity in rodents and non-human primates, by producing long-term depletion of dopamine (DA) and its metabolite, 3,4-dihydroxyphenylacetic acid (DOPAC), as well as reducing the density of DA transporter (DAT) in the striatum (Davidson et al. 2001; Cadet et al. 2003; Fukami et al. 2004; Koike et al. 2005; Zhang et al. 2006; Hashimoto et al. 2004; 2007; Hagiwara et al. 2009). Furthermore, it has been reported that levels of dopamine nerve terminal markers, DA, tyrosine hydroxylase, and DAT are decreased in the striatum of post mortem brains (nucleus accumbens, caudate, putamen) of chronic METH users (Wilson et al. 1996). Moreover, brain imaging studies using PET show that the density of DAT in the caudate/putamen and nucleus accumbens of METH users is significantly lower than that of healthy controls (Sekine et al. 2001; Volkow et al. 2001). Although METH-induced neurotoxicity at dopaminergic terminals is well documented, the precise mechanisms of METH-induced neurotoxicity remain unknown (Cadet et al. 2003; Hashimoto 2007; Chen et al. 2010).

Multiple lines of evidence implicate oxidative stress in the METH-induced behavioral and neuropathological changes that damage brain dopaminergic neurons (Açikgöz et al. 2001; Fukami et al. 2004; Miyazaki et al. 2006; Hashimoto et al. 2004, 2007; Cadet et al. 2007; Yamamoto and Raudensky 2008; Chen et al. 2010). The potent antioxidant sulforaphane (SFN: 1-isothiocyanato-4-methylsulfinylbutane) is an organosulfur compound derived from a glucosinolate precursor found in cruciferous vegetables such as broccoli, Brussels sprouts, and cabbage (Zhang et al. 2005; Juge et al. 2007). A number of studies show that SFN is a very potent chemopreventative agent in numerous animal carcinogenesis and cell culture models (Juge et al. 2007; Cheung and Kong 2010; Kwak and Kensler 2010). The protection afforded by SFN is thought to be mediated via activation of the NF-E2-related factor-2 (Nrf2) pathway and subsequent up-regulation of phase II detoxification enzymes and antioxidant proteins, through an enhancer sequence referred to as the electrophilic responsive element or antioxidant responsive element (ARE) (Itoh et al. 2004; Kang et al. 2005; Cheung and Kong 2010; Kwak and Kensler 2010). Furthermore, SFN is known to exert neuroprotective effects against neurotoxicity caused by 6-hydroxydopamine, tetrahydrobiopterin, and ischemia/reperfusion, again through activation of the Nrf2–ARE pathway (Han et al. 2007; Danilov et al. 2009; Siebert et al. 2009; Ping et al. 2010). It has been reported that SFN increases Nrf2 protein levels in the striatum and affords protection against methyl-4-phenyl-1,2,3,6-tetrahydropyridine (MPTP)-induced death of nigral dopaminergic neurons (Jazwa et al. 2011). Taken together, it is likely that as a potent Nrf2 activator, SFN could protect against the death of dopaminergic neurons in the brains of Parkinson's disease patients suffering from oxidative stress-related neuropsychiatric diseases.

Given the potent antioxidant effects of SFN, it is of interest to determine whether SFN can attenuate behavioral and neuropathological changes associated with METH exposure. In this study, we investigated the effects of SFN on acute hyperlocomotion and the development of behavioral sensitization induced by the administration of METH. We also examined the effects of SFN on METH-induced neurotoxicity in the dopaminergic neurons of the mouse striatum.

Materials and methods

Animals

Male Balb/c AnNCrlCrlj (8 weeks old, 23–30 g body weight at the beginning of the experiment; Charles River Japan Inc., Tokyo, Japan) mice were housed under a 12-h light/12-h dark cycle (lights on from 07:00 to 19:00 hours) at room temperature (22±2°C; humidity, 55±5%) with free access to food and water. Balb/c mice were used, since this strain has a known sensitivity to METH-induced neurotoxicity (Kita et al. 1998; Koike et al. 2005; Zhang et al. 2006; Hagiwara et al. 2009). Experimental protocols were approved by the Institutional Animal Care and Use Committee of Chiba University.

Drugs

METH hydrochloride (d-methamphetamine; Dainippon Pharmaceutical Ltd., Osaka, Japan) was dissolved in physiological saline, and (*R*,*S*)-sulforaphane (SFN) (LKT Laboratories, Inc., St Paul, MN, USA) was dissolved in distilled water including 10% corn oil. All other chemicals were purchased from commercial sources. The dose of METH was expressed as a hydrochloride salt.

Behavioral evaluations

Effects of SFN on hyperlocomotion after a single administration of METH

In the acute behavioral experiments, the initial period of acclimation was 60 min. Either vehicle (10 ml/kg) or SFN at 1, 3, or 10 mg/kg was administered intraperitoneally (i.p.) to mice. Thirty minutes after the first injection, mice were injected subcutaneously (s.c.) with METH (3.0 mg/kg) or vehicle (10 ml/kg). Locomotor activity was measured over 3.5 h using an animal movement analysis system (SCANET SV-10; Melquest, Toyama, Japan), as reported previously (Zhang et al. 2006; Hagiwara et al. 2009).

Effects of SFN on the development of behavioral sensitization after repeated administration of METH

Forty mice were divided into the following four groups: a vehicle (10 ml/kg, i.p.)+vehicle (10 ml/kg, s.c.) group; a vehicle (10 ml/kg, i.p.)+METH (3 mg/kg, s.c.) group; a SFN (10 mg/kg, i.p.)+METH (3 mg/kg, s.c.) group; and a SFN (10 mg/kg, i.p.)+vehicle (10 ml/kg, s.c.) group. The interval between the first pretreatment injection and second test injection was 30 min. In this study, we used a 10-mg/kg dose of SFN in mice, as this was the most effective dose in the METH-induced hyperlocomotion experiments. After the second test injection, mice were returned to their home cages. This cycle of injections was repeated for each animal, on five consecutive days. One week after the final treatment, each mouse was given a low dose of METH (1 mg/kg, s.c.), and locomotion was measured over 3 h (including 1 h habituation) using an animal movement analysis system (SCANET SV-10), as described above (Zhang et al. 2006; Hagiwara et al. 2009).

METH-induced dopaminergic neurotoxicity in the striatum

We examined the effects of pretreatment and subsequent treatment with SFN on METH-induced neurotoxicity in mice. Thirty minutes after pretreatment injections of SFN (10 mg/kg, i.p.) or vehicle (10 ml/kg, i.p.), mice received three injections of METH (3 mg/kg, s.c.) or vehicle (10 ml/kg, s.c.) at 3-h intervals. Rectal temperatures were measured using a TD-320 thermometer coupled to a rectal probe (Shibaura Electronics Co., Ltd., Saitama, Japan), and temperatures were recorded 30 min before pretreatment injections and at 1, 4, and 7 h after the first injection of METH. Then, vehicle (10 ml/kg, i.p.) or SFN (10 mg/kg, i.p.) was administered to the mice 12 h after the first administration of vehicle or SFN (day 1). The mice received two daily (12-h intervals) injections of SFN (10 mg/kg, i.p.) or vehicle (10 ml/kg, i.p.) for two consecutive days (days 2 and 3). In this experiment, we used a treatment schedule to examine both prophylactic and therapeutic effects of SFN. Mice were sacrificed 3 days after the administration of METH for the measurement of DA and DOPAC levels. The brains were quickly removed and the striatum was dissected away on an ice-cold glass plate. Samples were stored at −80°C until use.

Measurement of DA and DOPAC by HPLC

Levels of DA and DOPAC in the mouse striatum were measured using high performance liquid chromatography (HPLC), coupled with electrochemical detection as reported previously (Koike et al. 2005; Zhang et al. 2006; Hagiwara et al. 2009). Briefly, tissue samples were homogenized in 0.2 M perchloric acid ($HClO_4$), containing 100 μM disodium EDTA and 100 ng/ml isoproterenol (internal standard), and were then centrifuged at 20,000×*g* for 15 min at 4°C. Supernatants were filtered through a 0.45-μm pore membrane (Millex-LH, 4 mm; Millipore, Tokyo, Japan). The HPLC system consisted of a liquid chromatograph pump (EP-300, Eicom, Kyoto, Japan), a degasser (DG-300, Eicom), a reversed phase column (Eicompak SC-5ODS 3.0×150 mm; Eicom), an ECD-300 electrochemical detector (Eicom), and a data processor (EPC-300, Eicom). The mobile phase consisted of 0.1 M acetate–citric acid buffer (pH 3.5) containing 16% methanol, 5 mg/l disodium EDTA, and 190 mg/l sodium octyl sulfate.

Immunohistochemistry for DAT and MAC1 in the brain

Immunohistochemistry on the mouse brain sections was performed as reported previously (Koike et al. 2005; Zhang et al. 2006; Hagiwara et al. 2009). Three days after the administration of METH (3 mg/kg×3 at 3-h intervals), mice were anesthetized with sodium pentobarbital (50 mg/kg) and perfused transcardially with 10 ml of isotonic saline, followed by 40 ml of ice-cold, 4% paraformaldehyde in 0.1 M phosphate buffer (pH 7.4). Brains were removed from the skulls and postfixed overnight at 4°C in the same fixative. For the immunohistochemical analysis, 50-μm-thick serial, coronal sections of brain tissue were cut in ice-cold, 0.01 M phosphate buffered saline (pH 7.5) using a vibrating blade microtome (VT1000S, Leica Microsystems AG, Wetzlar, Germany). Free-floating sections were treated with 0.3% H_2O_2 in 50 mM Tris–HCl saline (TBS) for 30 min and were blocked in TBS containing 0.2% Triton X-100 (TBST) and 1.5% normal serum for 1 h at room temperature. The samples were then incubated for 36 h at 4°C with rat anti-DAT antibody (1:10,000, Cat. no: MAB 369, Chemicon International Inc., Temecula, CA, USA) or rat anti-MAC1 (CD11b; activated microglia) antibody (1:1,000, Cat. no: MCA74G, Serotec Ltd., Oxford, UK). The sections were washed twice in TBS and then processed using the avidin–biotin–peroxidase method (Vectastain Elite ABC,

Vector Laboratories, Inc., Burlingame, CA, USA). Sections were incubated for 5 min in a solution of 0.15 mg/ml diaminobenzidine containing 0.01% H_2O_2. Then, sections were mounted on gelatinized slides, dehydrated, cleared, and coverslipped under Permount® (Fisher Scientific, Fair Lawn, NJ, USA). The sections were imaged, and the staining intensity of DAT immunoreactivity in the anterior regions of the striatum was analyzed using a light microscope equipped with a CCD camera (Olympus IX70) and the SCION IMAGE software package. MAC1 immunoreactivity was quantified in the anterior regions (0.018 mm^2) of the striatum, in a blinded manner.

Statistical analysis

Data are presented as the mean±standard error of the mean (SEM). The results of the behavioral study and rectal temperature measurements were analyzed by two-way analysis of variance (ANOVA) for repeated measures, with treatment as the between-subjects factor and time as the within-subjects factor. When appropriate, group means at individual time points were compared by one-way ANOVA, and post hoc comparisons were performed using the Bonferroni/Dunn test. Levels of DA and DOPAC, as well as the densities of DAT immunoreactivity and MAC1 (activated microglia)-immunoreactive staining cells and the behavioral study, were analyzed by one-way ANOVA, followed by the post hoc Bonferroni/Dunn test for multiple comparisons. For all analyses, p values of less than 0.05 were considered statistically significant.

Results

Effects of SFN on hyperlocomotion in mice after a single administration of METH

A single administration of METH (3 mg/kg, s.c.) markedly increased locomotion in mice. Two-way ANOVA analysis revealed significant differences among the six groups studied [F (5, 100)=11.18, p<0.0001]. Pretreatment with SFN (at 1, 3, or 10 mg/kg, i.p., 30 min before the administration of METH) attenuated METH-induced hyperlocomotion in mice, in a dose-dependent manner (Fig. 1). High dose of SFN (10 mg/kg) significantly attenuated METH-induced hyperlocomotion in mice (Fig. 1). In contrast, SFN (10 mg/kg) alone did not alter locomotion in mice when compared to vehicle controls (Fig. 1).

Effects of SFN on the development of behavioral sensitization after repeated administration of METH

Repeated administration of METH (3 mg/kg/day, once daily for five consecutive days) increased METH (1 mg/kg)-induced hyperlocomotion in mice previously treated with METH, compared with the results obtained from the control (vehicle+vehicle) group. These results indicated the development of behavioral sensitization by repeated treatment with METH (Fig. 2). Two-way ANOVA analysis revealed significant differences among the four groups [F (3, 51)= 5.22, p<0.001]. The post hoc analysis showed that repeated

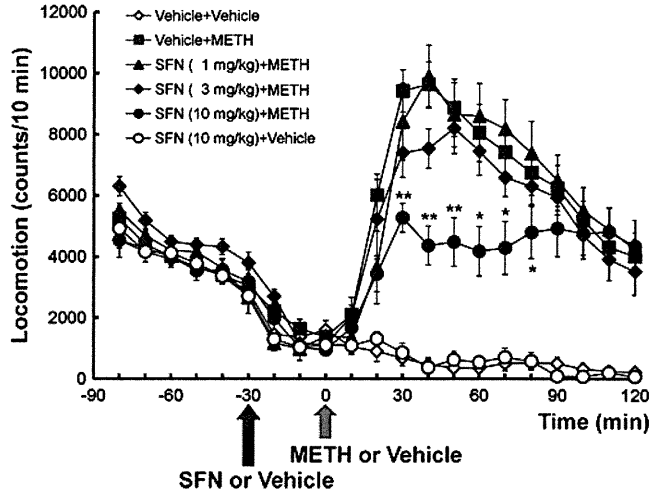

Fig. 1 Effects of SFN on hyperlocomotion in mice after a single administration of METH. Thirty minutes after i.p. injection of vehicle (10 ml/kg) or SFN (1, 3, or 10 mg/kg), METH (3 mg/kg) or vehicle (10 ml/kg) was administered s.c. to the mice. Behavior (locomotion) in the mice was evaluated. Each value is the mean±SEM (n=10–11 per group). *p<0.05, **p<0.01 as compared with the vehicle+METH group (Bonferroni/Dunn method)

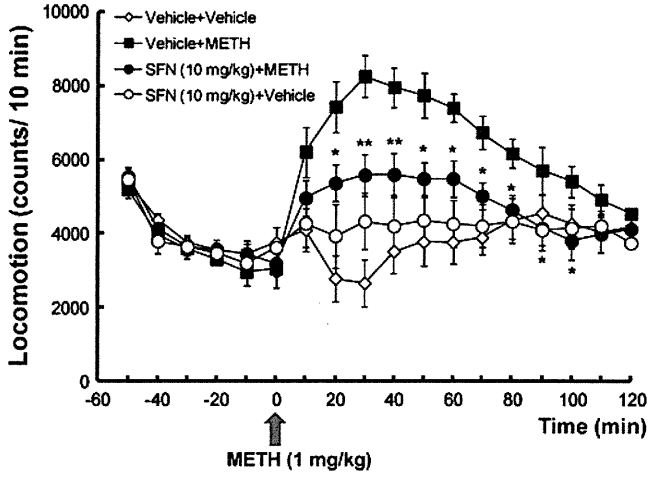

Fig. 2 Effects of SFN on the development of behavioral sensitization in mice after the repeated administration of METH. Vehicle (10 ml/kg)+vehicle (10 ml/kg) group, vehicle (10 ml/kg)+METH (3 mg/kg) group, SFN (10 mg/kg)+METH (3 mg/kg) group, and SFN (10 mg/kg)+vehicle (10 ml/kg) group were treated daily as noted for five consecutive days. Seven days after the final administration of METH, a lower dose of METH (1 mg/kg, s.c.) was administered to all mice. Behavior (locomotion) in the mice was evaluated. Each value is the mean±SEM (n=10 per group). *p<0.05, **p<0.01 as compared to the vehicle+METH group (Bonferroni/Dunn method)

administration of METH significantly ($p<0.001$) increased METH (1 mg/kg)-induced hyperlocomotion in mice previously treated with METH, compared with the control group. The post hoc analysis also showed that pretreatment with SFN (10 mg/kg) significantly [F (3, 27)=6.13, $p<0.05$] attenuated the development of sensitization after the administration of METH. In contrast, locomotion in the SFN (10 mg/kg)+vehicle group did not differ from that of the control (vehicle+vehicle) group (Fig. 2).

Effects of SFN on hyperthermia induced by the administration of METH

Two-way ANOVA analysis revealed significant differences among the four groups [F (3, 9)=38.51, $p<0.0001$]. Repeated injections of METH (3 mg/kg×3 at 3-h intervals) produced significant hyperthermia in these mice (Fig. 3). However, pretreatment with SFN (10 mg/kg) did not affect the induction of METH-induced hyperthermia in the mice (Fig. 3). Furthermore, SFN (10 mg/kg) alone did not alter rectal temperatures in these mice.

Effects of SFN on the reduction in DA and DOPAC levels in the striatum by the repeated administration of METH

One-way ANOVA analysis revealed that striatal DA [F (3, 38)=12.95, $p<0.0001$] and DOPAC [F (3, 38)=5.60, $p=0.0028$] levels were significantly different among the four groups studied. Pretreatment and a subsequent dose of SFN (10 mg/kg) significantly attenuated the reduction of DA and DOPAC in the striatum typically observed after repeated administration of METH (Fig. 4). Furthermore, treatment

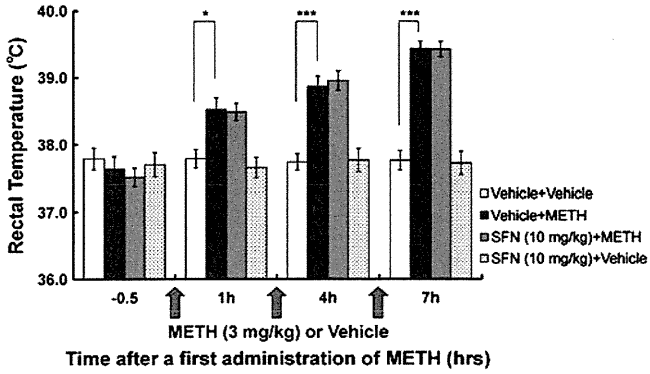

Fig. 3 Effect of SFN on METH-induced hyperthermia in mice. Mice received three injections of vehicle (10 ml/kg, 3-h intervals, s.c.) or METH (3 mg/kg, 3-h intervals, s.c). Vehicle (10 ml/kg, i.p.) or SFN (10 mg/kg, i.p.) was injected into the mice 30 min prior the first injection of METH or vehicle. Rectal temperature was recorded 30 min before the first injection of METH or vehicle and 1, 4, or 7 h after the first METH (or vehicle) injection. Each value is the mean± SEM (n=8–9 per group). *$p<0.05$, ***$p<0.001$ as compared to the vehicle+METH group (Bonferroni/Dunn method)

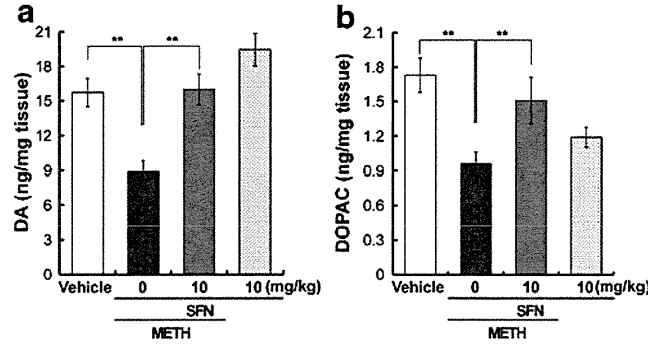

Fig. 4 Effects of SFN on DA (**a**) and DOPAC (**b**) levels in the mouse striatum after the repeated administration of METH. Thirty minutes after i.p. injection of SFN (10 mg/kg) or vehicle (10 ml/kg), mice received three injections of METH (3 mg/kg, s.c.) or vehicle (10 ml/kg, s.c.) at 3-h intervals (day 1). Then, vehicle (10 ml/kg, i.p.) or SFN (10 mg/kg, i.p.) was administered to the mice 12 h after the first administration of vehicle or SFN (day 1). Mice received two daily (12-h intervals) injections of SFN (10 mg/kg, i.p.) or vehicle (10 ml/kg, i.p.) for two consecutive days (days 2 and 3). Mice were sacrificed 3 days after the administration of METH (day 4). Values are the mean±SEM (n=10–11 per group). **$p<0.01$ as compared to the vehicle+METH group (Bonferroni/Dunn method)

with SFN (10 mg/kg) alone did not alter levels of DA and DOPAC in the mouse striatum (Fig. 4).

DAT immunohistochemistry

Repeated administration of METH (3 mg/kg×3 at 3-h intervals) markedly decreased the density of DAT in the mouse striatum (Fig. 5). One-way ANOVA analysis showed significant differences in DAT immunoreactivity in the striatum [F (3, 30)=55.93, $p<0.0001$] among the four groups. The post hoc analysis indicated that pretreatment and subsequent administration of SFN (10 mg/kg) significantly ($p<0.0001$) attenuated the reduction of DAT immunoreactivity in the mouse striatum usually seen after repeated administration of METH (Fig. 5). The administration of SFN (10 mg/kg) alone did not alter the density of DAT immunoreactivity in the mouse striatum (Fig. 5).

MAC1 immunohistochemistry

Three days after the repeated dose of METH (3 mg/kg×3 at 3-h intervals), MAC1 immunoreactivity in the mouse striatum was markedly increased (Fig. 6). One-way ANOVA analysis revealed significant differences among the four groups [F (3, 31)=277.41, $p<0.0001$], and the post hoc analysis showed that pretreatment and a subsequent administration of SFN (10 mg/kg) significantly ($p<0.001$) attenuated the increase in MAC1 immunoreactivity in the striatum associated with the administration of METH. Treatment with SFN (10 mg/kg) plus vehicle had no effect on MAC1 immunoreactivity in the mouse striatum (Fig. 6).

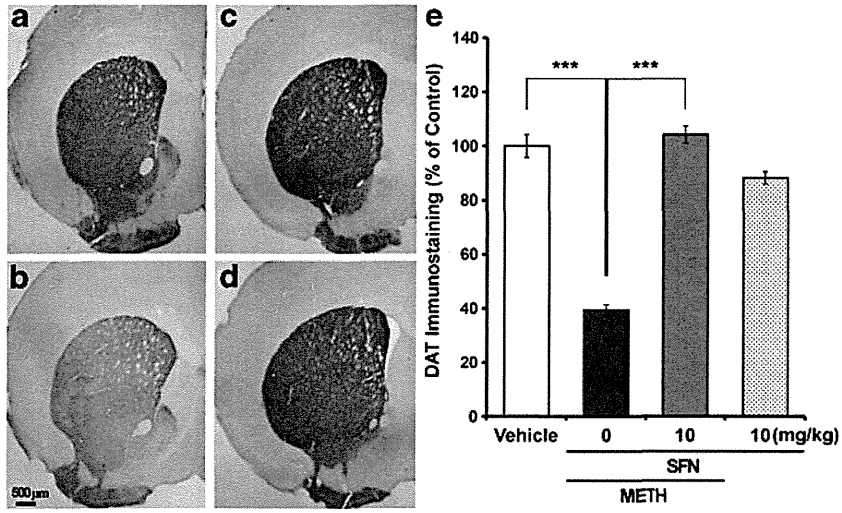

Fig. 5 Effects of SFN on the reduction of DAT density in the mouse striatum after repeated administration of METH. **a** Vehicle+vehicle, **b** vehicle+METH, **c** SFN+METH, and **d** SFN+vehicle. Thirty minutes after i.p. injection of SFN (10 mg/kg) or vehicle (10 ml/kg), the mice received three injections of METH (3 mg/kg, s.c.) or vehicle (10 ml/kg, s.c.) at 3-h intervals (day 1). Then, vehicle (10 ml/kg, i.p.) or SFN (10 mg/kg, i.p.) was administered to the mice 12 h after the first administration of vehicle or SFN (day 1). The mice received two daily (12-h intervals) injections of SFN (10 mg/kg, i.p.) or vehicle (10 ml/kg, i.p.) for two consecutive days (days 2 and 3). The mice were perfused 3 days after the administration of METH (day 4). **a–d** Representative photomicrographs showing the DAT immunoreactivity in the striatum of the mice. *Scale bar* was 500 μm. The mean value for DAT immunoreactivity staining was determined for each group and was expressed as a percentage of that of matched control group (**e**). Each value is the mean±SEM (n=7–9 per group). ***p<0.001 as compared to the vehicle+METH group (Bonferroni/Dunn method)

Discussion

A major finding of this study is that SFN ameliorated behavioral changes such as acute hyperlocomotion and the development of behavioral sensitization typically induced by the administration of METH. It also showed that SFN protects against METH-induced dopaminergic neurotoxicity in the mouse striatum. SFN occurs naturally in cruciferous vegetables like broccoli, cabbage, watercress, and Brussels sprouts, in its precursor form, glucosinolate. On chewing, the glucose moiety of this glucosinolate precursor is hydrolyzed by myrosinase into the corresponding isothiocyanate (Fenwick et al. 1983). Interestingly, dietary SFN-rich sprouts reduce colonization and attenuate gastritis in *Helicobacter pylori*-infected humans (Yanaka et al. 2009; Yanaka 2011). In addition, a phase II study of SFN (200 μmol (35 mg) daily) in patients with recurrent prostate cancer is now in progress (NCT01228084). Taken together, our results suggest that SFN could be a promising, therapeutic drug for the treatment of multiple signs associated with METH abuse in humans, particularly as it is safe for human consumption.

The acute pharmacological effects of amphetamines such as METH are linked to their capacity to increase extracellular DA levels via the release of DA from presynaptic terminals and by the inhibition of DA re-uptake (Seiden et al. 1993). In this study, we found that pretreatment with SFN attenuated acute hyperlocomotion in mice, induced by a single dose of METH. This study does not identify the precise cellular mechanisms for the actions of SFN on METH-induced behavioral effects; however, the findings at least in part suggest that SFN acts by decreasing extracellular DA levels in the mouse striatum. SFN is widely reported to induce Nrf2-dependent gene expression, although its molecular targets have not been fully characterized (Juge et al. 2007; Cheung and Kong 2010; Kwak and Kensler 2010). It remains unclear as to whether activation of the Nrf-2-electrophile-responsive element/ARE pathway accounts for the ability of SFN to diminish the acute behavioral effects induced by METH in mice. Further studies on the ability of this agent to ameliorate METH-associated acute neurochemical and behavioral effects will be necessary.

Repeated exposure to METH results in a progressively enhanced and enduring behavioral response to the drug, a phenomenon known as behavioral sensitization. A number of behavioral, neurochemical, biochemical, and molecular studies have shown that the initiation of this complex process involves the interaction of several neurotransmitters, neuropeptides, neurotrophic factors, and their associated receptor signaling pathways (Robinson and Becker 1986; Pierce and Kalivas 1997; White and Kalivas 1998; Licata and Pierce 2003; Vanderschuren and Kalivas 2000; Scholl et al. 2009). Determining the full interplay of these factors remains elusive. Several studies propose the involvement of the mesolimbic dopamine system, including the ventral tegmental area, nucleus accumbens, and associated brain regions such as the striatum in the development of behavioral sensitization. Previously, we reported that antioxidants

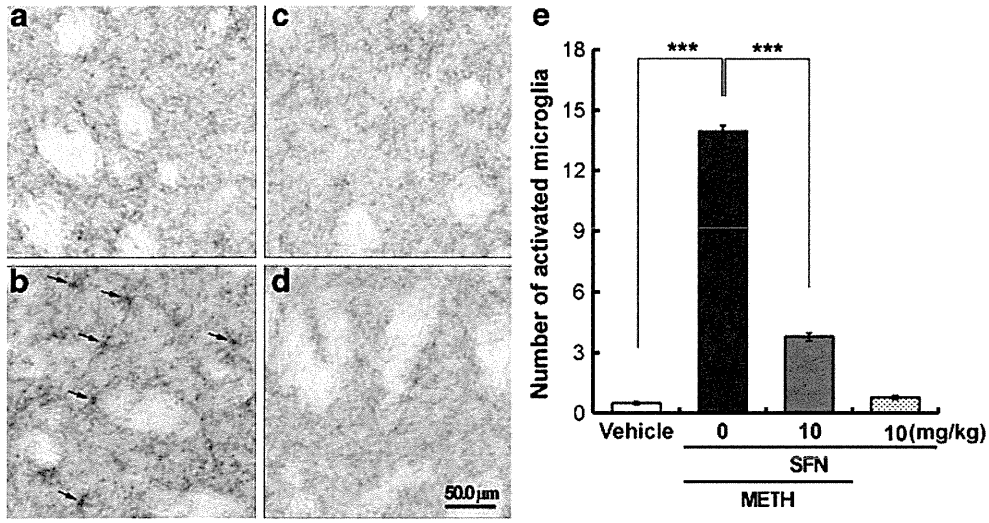

Fig. 6 Effects of SFN on microglial activation in the mouse striatum after the repeated administration of METH. **a** Vehicle+vehicle, **b** vehicle+METH, **c** SFN+METH, and **d** SFN+vehicle. Thirty minutes after i.p. injection of SFN (10 mg/kg) or vehicle (10 ml/kg), the mice received three injections of METH (3 mg/kg, s.c.) or vehicle (10 ml/kg, s.c.) at 3-h intervals (day 1). Then, vehicle (10 ml/kg, i.p.) or SFN (10 mg/kg, i.p.) was administered to the mice 12 h after the first administration of vehicle or SFN (day 1). The mice received two daily (12-h intervals) injections of SFN (10 mg/kg, i.p.) or vehicle (10 ml/kg, i.p.) for two consecutive days (days 2 and 3). Mice were perfused 3 days after the administration of METH (day 4), and MAC1 immunohistochemistry was performed. **a**–**d** Representative photomicrographs depicting MAC1 immunoreactivity (activated microglia) in the striatum of mice. Resting state microglia was observed in the striatum of the control mice (**a**). Activated microglia was observed in the striatum of METH-treated mice (**b**). *Scale bar* was 50 μm. The mean value representing the staining of activated microglia was determined for each group and was expressed as a percentage of that of matched control mice (**c**). The number of activated microglia was counted based on one microscopic view (×200) (**e**). Each value is the mean±SEM (n=8–9 per group). ***p<0.001 as compared to vehicle+METH group (Bonferroni/Dunn method)

such as *N*-acetyl-L-cysteine and minocycline attenuate the development of METH-induced behavioral sensitization in rodents (Fukami et al. 2004; Zhang et al. 2006). It is therefore likely that the potent antioxidant properties of SFN play a role in its actions, although further detailed studies are needed to confirm this.

In this study, we found that pretreatment and subsequent administration of SFN (10 mg/kg) significantly attenuated the METH-induced reduction of DA and DOPAC levels as well as DAT immunoreactivity in the mouse striatum. These protective mechanisms may block the neurotoxic effects on DA neurons. Further studies will still be necessary to fully define these mechanisms. In the treatment paradigm of METH-induced neurotoxicity (3 mg/kg×3 at 3-h intervals), we performed behavioral evaluations in mice after three injections of METH. We found that behavioral abnormalities in mice after the first administration of METH are similar to the results (Fig. 1) of acute METH administration (Supplemental Fig. 1). In contrast, we found that behavioral abnormalities in mice after the third administration of METH were similar between the groups, vehicle+METH and SFN+METH, indicating that the effect of SFN was not detectable in behavioral abnormalities after the third administration of METH (Supplemental Fig. 1). Thus, it is unlikely that the biochemical effects of SFN on METH-induced neurotoxicity are similar to the behavioral effects of SFN on METH-induced behavioral abnormalities.

A number of studies show that the METH-induced neurotoxic effect on DA nerve endings within the striatum is associated with microglial activation (Escubedo et al. 1998; Pubill et al. 2003; Guilarte et al. 2003; LaVoie et al. 2004; Thomas et al. 2004; Thomas and Kuhn 2005; Zhang et al. 2006). The temporal and dosage relationships between METH-induced neurotoxicity and microglial activation suggest that this activation might contribute to METH-induced neurotoxicity in the striatum (Thomas et al. 2004). Interestingly, SFN reduces lipopolysaccharide-induced microglial activation in the mouse brain, suggesting that SFN is a potent inhibitor of microglial activation (Innamorato et al. 2008). We conclude that, in part, SFN reduces METH-induced neurotoxicity in the mouse striatum by inhibiting microglial activation. Additional studies on the role of microglial activation in METH-induced dopaminergic neurotoxicity are warranted.

A number of studies indicate that neurotoxic doses of METH cause hyperthermia and that hypothermia can suppress METH-induced neurotoxicity, suggesting a role for body temperature in METH-induced dopaminergic neurotoxicity (Albers and Sonsalla 1995; Ali et al. 1996). However, we found no evidence that SFN altered METH-induced hyperthermia in mice. Therefore, it is unlikely that body temperature plays a role in the protective effect of SFN on METH-induced neurotoxicity in mice.

Recently, it has been reported that SFN increases Nrf2 protein levels in the mouse striatum and protects against MPTP-induced death of nigral dopaminergic neurons in a cell culture model of Parkinson's disease (Jazwa et al. 2011). In the neonatal hypoxia–ischemia rat model, pretreatment with SFN increases the expression of Nrf2 immunoreactivity, while decreasing the number of TUNEL-positive neurons and microglial activation in the rat brain (Ping et al. 2010), suggesting that its neuroprotective effect is mediated through increased Nrf2 expression. It is likely that SFN protects against dopaminergic neurotoxicity in the mouse striatum by increasing Nrf2 expression, although this needs to be confirmed.

In conclusion, this study demonstrated that in mice, SFN inhibited METH-induced behavioral changes such as acute hyperlocomotion and the development of behavioral sensitization and dopaminergic neurotoxicity in mice. This makes SFN a promising therapeutic agent for the treatment of multiple signs associated with METH abuse, since it is a naturally occurring compound found in cruciferous vegetables.

Acknowledgment This study is supported partly by a grant from Intramural Research Grant (22-2: to K.H.) for Neurological and Psychiatric Disorders of NCNP, Japan.

Conflicts of interest All authors had no potential conflict of interest.

References

Açikgöz O, Gonenc S, Gezer S et al (2001) Methamphetamine causes depletion of glutathione and an increase in oxidized glutathione in the rat striatum and prefrontal cortex. Neurotox Res 3:277–280

Albers DS, Sonsalla PK (1995) Methamphetamine-induced hyperthermia and dopaminergic neurotoxicity in mice: pharmacological profile of protective and nonprotective agents. J Pharmacol Exp Ther 275:1104–1114

Ali SF, Newport GD, Slikker W Jr (1996) Methamphetamine-induced dopaminergic toxicity in mice. Role of environmental temperature and pharmacological agents. Ann NY Acad Sci 801:187–198

Barr A, Panenka W, MacEwan W et al (2006) The need for speed: an update on methamphetamine addiction. J Psychiatry Neurosci 31:301–313

Cadet JL, Jayanthi S, Deng X (2003) Speed kills: cellular and molecular bases of methamphetamine-induced nerve terminal degeneration and neuronal apoptosis. FASEB J 17:1775–1788

Cadet JL, Krasnova IN, Jayanthi S, Lyles J (2007) Neurotoxicity of substituted amphetamines: molecular and cellular mechanisms. Neurotox Res 11:183–202

Chen HX, Wu J, Zhang JC, Hashimoto K (2010) Recent topics on pharmacotherapy for amphetamine-type stimulants abuse and dependence. Curr Drug Abuse Rev 3:222–238

Cheung KL, Kong AN (2010) Molecular targets of dietary phenylethyl isothiocyanate and sulforaphane for cancer chemoprevention. AAPS J 12:87–97

Colfax G, Santos GM, Chu P et al (2010) Amphetamine-group substances and HIV. Lancet 376:458–474

Danilov CA, Chandrasekaran K, Racz J, Soane L, Zielke C, Fiskum G (2009) Sulforaphane protects astrocytes against oxidative stress and delayed death caused by oxygen and glucose deprivation. Glia 57:645–656

Davidson C, Gow AJ, Lee TH, Ellinwood EH (2001) Methamphetamine neutoxicity: necrotic and apoptotic mechanisms and relevance to human abuse and treatment. Brain Res Rev 6:1–22

Escubedo E, Guitart L, Sureda FX et al (1998) Microgliosis and downregulation of adenosine transporter induced by methamphetamine in rats. Brain Res 814:120–126

Fenwick GR, Heaney RK, Mullin WJ (1983) Glucosinolates and their breakdown products in food and food plants. Crit Rev Food Sci Nutr 18:123–201

Fukami G, Hashimoto K, Koike K, Okamura N, Shimizu E, Iyo M (2004) Effect of antioxidant *N*-acetyl-L-cysteine on behavioral changes and neurotoxicity in rats after administration of methamphetamine. Brain Res 1016:90–95

Gonzales R, Mooney L, Rawson RA (2010) The methamphetamine problem in the United States. Annu Rev Public Health 31:385–398

Guilarte TR, Nihei MK, McGlothan JL, Howard AS (2003) Methamphetamine induced deficits of brain monoaminergic neuronal markers: distal axotomy or neuronal plasticity. Neuroscience 122:499–513

Hagiwara H, Iyo M, Hashimoto K (2009) Mithramycin protects against dopaminergic neurotoxicity in the mouse brain after administration of methamphetamine. Brain Res 1301:189–196

Han JM, Lee YJ, Lee SY et al (2007) Protective effect of sulforaphane against dopaminergic cell death. J Pharmacol Exp Ther 321:249–256

Hashimoto K (2007) New research on methamphetamine abuse. In: Toolaney GH (ed) New research on methamphetamine abuse. NovaScience, New York, pp 1–51

Hashimoto K, Tsukada H, Nishiyama S et al (2004) Protective effects of *N*-acetyl-L-cysteine on the reduction of dopamine transporters in the striatum of monkeys treated with methamphetamine. Neuropsychopharmacology 29:2018–2023

Hashimoto K, Tsukada H, Nishiyama S, Fukumoto D, Kakiuchi T, Iyo M (2007) Protective effects of minocycline on the reduction of dopamine transporters in the striatum after administration of methamphetamine: a PET study in conscious monkeys. Biol Psychiatry 61:577–581

Innamorato NG, Rojo AI, Garcia-Yagüe AJ, Yamamoto M, de Ceballos ML, Cuadrado A (2008) The transcription factor Nrf2 is a therapeutic target against brain inflammation. J Immunol 181:680–689

Itoh K, Tong KI, Yamamoto M (2004) Molecular mechanism activating Nrf2–Keap1 pathway in regulation of adaptive response to electrophiles. Free Radic Biol Med 36:1208–1213

Jazwa A, Rojo AI, Innamorato NG, Hesse M, Fernández-Ruiz J, Cuadrado A (2011) Pharmacological targeting of the transcription factor Nrf2 at the basal ganglia provides disease modifying therapy for experimental parkinsonism. Antioxid Redox Signal 14:2347–2360

Juge N, Mithen RF, Traka M (2007) Molecular basis for chemoprevention by sulforaphane: a comprehensive review. Cell Mol Life Sci 64:1105–1127

Kang KW, Lee SJ, Kim SG (2005) Molecular mechanism of nrf2 activation by oxidative stress. Antioxid Redox Signal 7:1664–1673

Kita T, Paku S, Takahashi M, Kubo K, Wagner GC, Nakashima T (1998) Methamphetamine-induced neurotoxicity in BALB/c, DBA/2 N and C57BL/6 N mice. Neuropharmacology 37:1177–1784

Koike K, Hashimoto K, Fukami G et al (2005) The immunophilin ligand FK506 protects against methamphetamine-induced dopaminergic neurotoxicity in mouse striatum. Neuropharmacology 48:391–397

Kwak MK, Kensler TW (2010) Targeting NRF2 signaling for cancer chemoprevention. Toxicol Appl Pharmacol 244:66–76

LaVoie MJ, Card JP, Hastings TG (2004) Microglia activation precedes dopamine terminal pathology in methamphetamine-induced neurotoxicity. Exp Neurol 187:47–57

Licata SC, Pierce RC (2003) The roles of calcium/calmodulin-dependent and Ras/mitogen-activated protein kinases in the development of psychostimulant-induced behavioral sensitization. J Neurochem 85:14–22

Miyazaki I, Asanuma M, Diaz-Corrales FJ et al (2006) Methamphetamine-induced dopaminergic neurotoxicity is regulated by quinone formation-related molecules. FASEB J 20:571–573

National Institute on Drug Abuse (2002) Research report series—methamphetamine abuse and addiction. NIDA, Rockville

Pierce RC, Kalivas PW (1997) A circuitry model of the expression of behavioral sensitization to amphetamine-like psychostimulants. Brain Res Rev 25:192–216

Ping Z, Liu W, Kang Z et al (2010) Sulforaphane protects brains against hypoxic–ischemic injury through induction of Nrf2-dependent phase 2 enzyme. Brain Res 1343:178–185

Pubill D, Canudas AM, Pallas M, Camins A, Camarasa J, Escubedo E (2003) Different glial response to methamphetamine- and methylenedioxymethamphetamine-induced neurotoxicity. Naunyn Schmiedebergs Arch Pharmacol 367:490–499

Robinson TE, Becker JB (1986) Enduring changes in brain and behavior produced by chronic amphetamine administration: a review and evaluation of animal models of amphetamine psychosis. Brain Res 396:157–198

Scholl JL, Feng N, Watt MJ, Renner KJ, Forster GL (2009) Individual differences in amphetamine sensitization, behavior and central monoamines. Physiol Behav 96:493–504

Seiden LS, Sabol KE, Ricaurte GA (1993) Amphetamine: effects on catecholamine systems and behavior. Annu Rev Pharmacol Toxicol 33:639–677

Sekine Y, Iyo M, Ouchi Y et al (2001) Methamphetamine-related psychiatric symptoms and reduced brain dopamine transporters studied with PET. Am J Psychiatry 158:1206–1214

Siebert A, Desai V, Chandrasekaran K, Fiskum G, Jafri MS (2009) Nrf2 activators provide neuroprotection against 6-hydroxydopamine toxicity in rat organotypic nigrostriatal cocultures. J Neurosci Res 87:1659–1669

Thomas DM, Kuhn DM (2005) Attenuated microglial activation mediates tolerance to the neurotoxic effects of methamphetamine. J Neurochem 92:790–797

Thomas DM, Walker PD, Benjamins JA, Geddes TJ, Kuhn DM (2004) Methamphetamine neurotoxicity in dopamine nerve endings of the striatum is associated with microglia activation. J Pharmacol Exp Ther 311:1–7

Ujike H, Sato M (2004) Clinical features of sensitization to methamphetamine observed in patients with methamphetamine dependence and psychosis. Ann NY Acad Sci 1025:279–287

United Nations Office on Drug Use and Crime (UNODC) (2008) World drug report. UNODC, Vienna

Vanderschuren LJ, Kalivas PW (2000) Alterations in dopaminergic and glutamatergic transmission in the induction and expression of behavioral sensitization: a critical review of preclinical studies. Psychopharmacology (Berl) 151:99–120

Volkow ND, Chang L, Wang GJ et al (2001) Association of dopamine transporter reduction with psychomotor impairment in methamphetamine abusers. Am J Psychiatry 158:377–382

White FJ, Kalivas PW (1998) Neuroadaptations involved in amphetamine and cocaine addiction. Drug Alcohol Depend 51:141–153

Wilson JM, Kalansinsky KS, Levey AI et al (1996) Striatal dopamine nerve terminal markers in human, chronic methamphetamine users. Nat Med 2:699–703

Yamamoto J (2004) Recent trends of drug abuse in Japan. Ann NY Acad Sci 1025:430–438

Yamamoto BK, Raudensky J (2008) The role of oxidative stress, metabolic compromise, and inflammation in neuronal injury produced by amphetamine-related drugs of abuse. J Neuroimmune Pharmacol 3:203–217

Yanaka A (2011) Sulforaphane enhances protection and repair of gastric mucosa against oxidative stress in vitro, and demonstrates anti-inflammatory effects on *Helicobacter pylori*-infected gastric mucosae in mice and human subjects. Curr Pham Des 17:1532–1540

Yanaka A, Fahey JW, Fukumoto A et al (2009) Dietary sulforaphane-rich broccoli sprouts reduce colonization and attenuate gastritis in *Helicobacter pylori*-infected mice and humans. Cancer Prev Res (Phila) 2:353–260

Zhang Y, Li J, Tang L (2005) Cancer-preventive isothiocyanates: dichotomous modulators of oxidative stress. Free Radic Biol Med 38:70–77

Zhang L, Kitaichi K, Fujimoto Y et al (2006) Protective effects of minocycline on behavioral changes and neurotoxicity in mice after administration of methamphetamine. Prog Neuro-Psychopharmacol Biol Psychiatry 30:1381–1393

BRAIN RESEARCH 1348 (2010) 200–208

available at www.sciencedirect.com

ScienceDirect

www.elsevier.com/locate/brainres

BRAIN RESEARCH

Research Report

Characterization of [^{3}H]CHIBA-1001 binding to α7 nicotinic acetylcholine receptors in the brain from rat, monkey, and human

Yuko Tanibuchi[a,b], *Jin Wu*[a], *Jun Toyohara*[a], *Yuko Fujita*[a], *Masaomi Iyo*[b], *Kenji Hashimoto*[a,*]

[a]*Division of Clinical Neuroscience, Chiba University Center for Forensic Mental Health, Chiba 260-8670, Japan*
[b]*Department of Psychiatry, Chiba University Graduate School of Medicine, Chiba 260-8670, Japan*

ARTICLE INFO

Article history:
Accepted 1 June 2010
Available online 9 June 2010

Keywords:
α7 nAChRs
Receptor binding
Rat brain
Monkey brain
Human brain

ABSTRACT

Accumulating evidence suggests that the α7 subtype of nicotinic acetylcholine receptors (nAChRs) plays a role in the pathophysiology of neuropsychiatric diseases, including schizophrenia and Alzheimer's disease. Currently, there are no suitable small molecule radioligands for α7 nAChRs in the brain, although [^{125}I]α-bungarotoxin has been widely used as a radioligand for α7 nAChRs. In the present study, we characterized a new radioligand, 4-[^{3}H]methylphenyl 2,5-diazabicyclo[3.2.2]nonane-2-carboxylate ([^{3}H]CHIBA-1001), a derivative of the selective α7 nAChR agonist SSR180711, in brain membranes from rat, monkey, and human. Scatchard analysis revealed an apparent equilibrium dissociation constant (Kd) of 193.4 nM in rat brain membranes at 4 °C, and the maximal number of binding sites (Bmax) was 346.2 fmol/mg protein. The order of drugs for the inhibition of [^{3}H]CHIBA-1001 binding to rat brain membranes is SSR180711>A-844606>MG624>epibatidine>DMAB>A-582941, suggesting a similarity of α7 nAChR pharmacological profiles. In contrast, α-bungarotoxin, MLA, and nicotine were found to be very weak. The distribution of [^{3}H]CHIBA-1001 binding to crude membranes from dissected regions of rat, monkey, and human brain was different from that of [^{125}I]α-bungarotoxin binding, suggesting that [^{3}H]CHIBA-1001 binding sites may not be identical to [^{125}I]α-bungarotoxin binding in the brain. In summary, [^{3}H]CHIBA-1001 would be a useful radioligand for α7 nAChRs in the brains of rodents, non-human primates, and humans.

1. Introduction

One of the subtypes of nicotinic acetylcholine receptors (nAChRs) is composed of α7 subunits, which are pentameric; this subtype is distinguished from other nAChRs by its relatively high permeability to Ca^{2+}, which rapidly activates and desensitizes ligand-gated ion channels expressed in the mammalian central nervous system. Accumulating evidence suggests that α7 nAChRs play a role in the pathophysiology of a number of neuropsychiatric diseases such as schizophrenia and Alzheimer's disease (Freedman et al., 1995; Simosky et al., 2002; Hashimoto and Iyo, 2002; Martin et al., 2004; Hashimoto et al., 2005; Olincy and Stevens, 2007; Adams and Stevens, 2007; Dziewczapolski et al., 2009; Wang et al., 2009; Toyohara and Hashimoto, 2010). Some studies using postmortem human brain samples have demonstrated alterations in the

* *Corresponding author.* Fax: +81 43 226 2561.
E-mail address: hashimoto@faculty.chiba-u.jp (K. Hashimoto).

0006-8993/$ – see front matter © 2010 Elsevier B.V. All rights reserved.
doi:10.1016/j.brainres.2010.06.008

levels of α7 nAChRs in the brains of patients with schizophrenia (Freedman et al., 1995; Marutle et al., 2001) and Alzheimer's disease (Hellström-Lindahl et al., 1999; Burghaus et al., 2000; Court et al., 2001; Wevers et al., 2000). In the brain, α7 nAChRs are widely expressed, with expression levels being particularly high in regions involved in cognitive processing, especially the hippocampus and cerebral cortex (Séguéla et al., 1993). Furthermore, animal studies using α7 nAChR knockout mice have demonstrated that α7 nAChRs might be involved in mediating the attentional effects of nicotine (Young et al., 2004, 2007). Moreover, a number of α7 nAChRs agonists such as PNU-282987 (Bodnar et al., 2005; Hajós et al., 2005), PHA-543613 (Wishka et al., 2006), AR-R17779 (Levin et al., 1999; Van Kampen et al., 2004), tropisetron (Hashimoto et al., 2006), SSR180711 (Pichat et al., 2007; Hashimoto et al., 2008a; Barak et al., 2009; Thomsen et al., 2009), and A-582941 (Bitner et al., 2007; Tietje et al., 2008) are reported to improve performance in animal models of cognitive deficits. It is therefore likely that α7 nAChR agonists are one of the potential therapeutic drugs for cognitive deficits in several neuropsychiatric diseases (Toyohara and Hashimoto, 2010).

It is, therefore, of great interest to determine whether α7 nAChRs are altered in the living brains of patients with these neuropsychiatric diseases. CHIBA-1001, 4-methylphenyl 2,5-diazabicyclo[3.2.2]nonane-2-carboxylate, is a derivative of the selective α7 nAChR agonist SSR180711 (Biton et al., 2007; Pichat et al., 2007) (Fig. 1). Previously, we reported that the IC_{50} values of SSR180711 and CHIBA-1001 for [^{125}I]a-bungarotoxin (0.5 nM) binding to the rat brain homogenates were 24.9 and 45.8 nM, respectively (Hashimoto et al., 2008b). Furthermore, CHIBA-1001 (1 μM) was found to be devoid of activity (inhibition lower than 50%) for a 28 standard receptor binding profile (Hashimoto et al., 2008b), indicating a high selectivity at α7 nAChRs. At present, it is not examined whether CHIBA-1001 is an agonist or an antagonist at α7 nAChRs. Recently, we have reported that [^{11}C]CHIBA-1001 might be a potential new positron emission tomography (PET) ligand for labeling in non-human primate (Hashimoto et al., 2008b) and human brain (Toyohara et al., 2009). Clinical PET studies using [^{11}C] CHIBA-1001 in patients with schizophrenia or Alzheimer's disease are currently underway (Toyohara et al., 2010). In addition, a number of new radioligands for α7 nAChRs, including [^{3}H]A-585539 (Anderson et al., 2008), [^{125}I]I-TSA (Ogawa et al., 2006), [^{11}C](R)-MeQAA (Ogawa et al., 2009), [^{11}C] GTS-21 (Kim et al., 2007), [^{18}F]NS10743 (Deuther-Conrad et al., 2009), [^{11}C]A-582941 and [^{11}C]A-844606 (Toyohara et al., 2010) have been reported (Toyohara et al., 2010). Although the radiolabeled peptide [^{125}I]α-bungarotoxin and the alkaloid [^{3}H]methyllycaconitine (MLA) have been widely used in *in vitro* receptor binding studies, these α7 nAChRs antagonists are substantially larger molecules than the endogenous agonists acetylcholine and choline. Detailed characterization of [^{3}H]CHIBA-1001 binding to brain membranes *in vitro* has not yet been reported, although a clinical study using [^{11}C] CHIBA-1001 has been started. In the present study, we performed a detailed characterization of [^{3}H]CHIBA-1001 binding to brain membranes from rat, non-human primate, and human. Furthermore, the regional distribution of [^{3}H] CHIBA-1001 binding in the brain was compared to that of [^{125}I]α-bungarotoxin binding.

2. Results

2.1. *Synthesis of [^{3}H]CHIBA-1001*

[^{3}H]CHIBA-1001 was synthesized by methylation of the precursor (Fig. 1). The radiochemical purity and specific activity of [^{3}H]CHIBA-1001 were approximately 99.2±0.4% (n=4) and 2960 GBq/mmol (based on the specific activity of [^{3}H]methyl iodide), respectively. The radiochemical yields of [^{3}H]CHIBA-1001 were 14.8±6.8% (n=4).

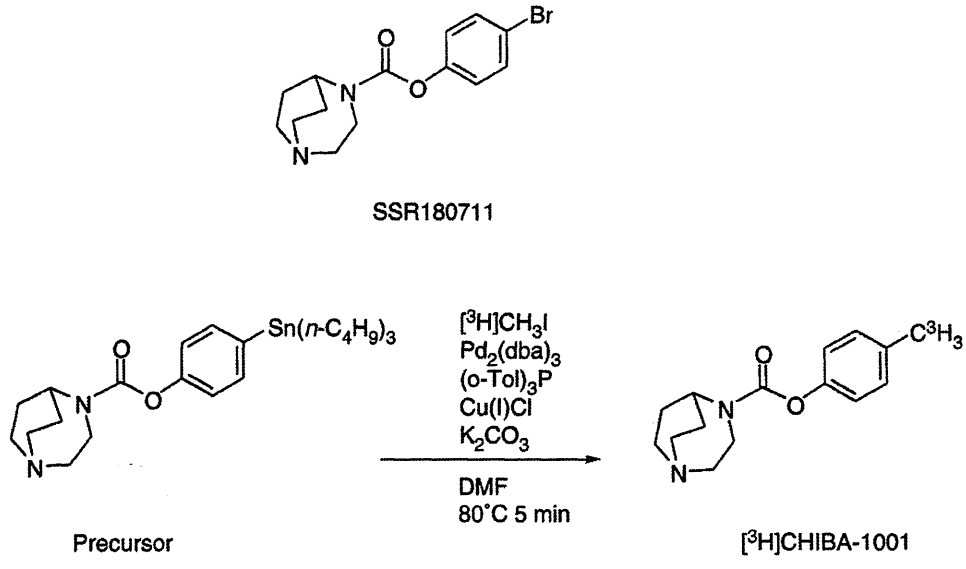

Fig. 1 – Synthesis of [^{3}H]CHIBA-1001. [^{3}H]CHIBA-1001 with a high specific activity was synthesized by *N*-methylation of the precursor, 4-(tributylstannyl)phenyl 2,5-diazabicyclo[3.2.2]nonane-2-carboxylate and [^{3}H]methyliodide.

2.2. *Equilibrium saturation binding of [^{3}H]CHIBA-1001 to rat brain membranes*

First, the kinetics of [^{3}H]CHIBA-1001 binding to rat brain membranes at 4 °C were studied. Specific binding reached equilibrium after 30 min (Supplemental Fig. 1). For saturation binding isotherms, six grade-diluted concentrations of [^{3}H] CHIBA-1001 (35–410 nM) were used. Specific binding of [^{3}H] CHIBA-1001 to rat brain membranes was saturable, and represented 40 to 50% of total binding over the concentration range examined (Fig. 2A). In saturation binding isotherms, nonlinear regression analysis of specific binding revealed an apparent Kd of 193.4±43.75 nM and a Bmax of 346.2±33.28 fmol/mg protein (n=3) at 4 °C (Fig. 2B). Nonspecific binding ranged from 15 to 50% of total binding for the range of [^{3}H]CHIBA-1001 concentrations.

2.3. *Pharmacological profiles of [^{3}H]CHIBA-1001 binding to rat brain membranes*

The pharmacological inhibition of specific [^{3}H]CHIBA-1001 (30 nM) binding to rat brain membranes was studied at 4 °C. Seven kinds of α7 nAChR compounds, including A-582941, PNU-282987, DMAB-anabaseine dihydrochloride, (±)-epibatidine, MG624, A-844606, and SSR180711, were found to displace [^{3}H] CHIBA-1001 binding to rat brain membranes (Fig. 3). The Ki value of SSR180711 was lowest, as expected, although epibatidine had low affinity at [^{3}H]CHIBA-1001 binding (Table 1). Other nAChR ligands such as (–)-nicotine, α-bungarotoxin, and MLA did not appear to inhibit [^{3}H]CHIBA-1001 binding to rat brain membranes.

2.4. *Regional distribution of [^{3}H]CHIBA-1001 binding in the rat brain*

Fig. 4 shows the regional distribution of specific bindings of [^{3}H] CHIBA-1001 in the rat brain, indicating no regional differences in [^{3}H]CHIBA-1001 binding. In contrast, regional distribution pattern of [^{125}I]α-bungarotoxin binding in the rat brain was similar to that reported previously (Davies et al., 1999). The binding of [^{125}I]α-bungarotoxin was relatively higher in the hippocampus and thalamus, while low binding density was shown in the cerebellum and striatum (Supplemental Figs. 2A and B). Furthermore, although the binding of [^{125}I]α-bungarotoxin to rat brain membranes was displaced by MLA, the binding of [^{3}H]CHIBA-1001 to rat brain membranes was not displaced by MLA (Table 1). In addition, specific binding of [^{125}I]α-bungarotoxin determined in the presence of SSR180711 and by MLA for nonspecific binding was very low in the striatum and cerebellum, although these data are preliminary (Supplemental Figs. 2A and B).

2.5. *Regional distribution of [^{3}H] CHIBA-1001 binding in the monkey brain*

The regional distribution of [^{3}H]CHIBA-1001 binding in the monkey brain was homogenous (Fig. 5). In contrast, regional

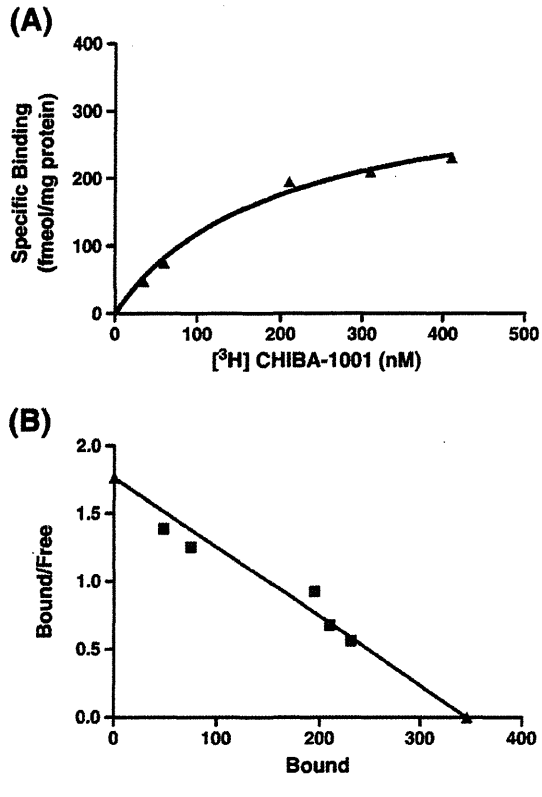

Fig. 2 – Specific binding of [^{3}H]CHIBA-1001 to rat brain membranes. Membranes were incubated with various concentrations of [^{3}H]CHIBA-1001 (35–410 nM) for 150 min at 4 °C. Nonspecific binding was estimated in the presence of 50 μM SSR180711. The results are from a typical experiment, and values are the average of duplicate determinations. (A) The saturation binding isotherm shows specific binding. (B) Scatchard plot analysis of [^{3}H]CHIBA-1001 binding gave a K_d of 193.4 nM and the B_{max} of 346.2 fmol/mg of protein.

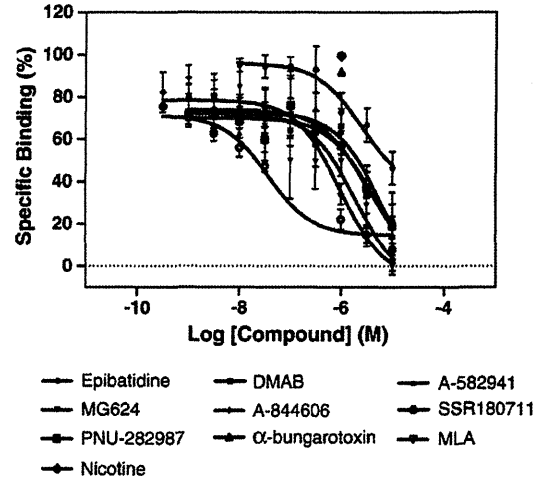

Fig. 3 – Competition curves of [^{3}H]CHIBA-1001 binding to rat brain membranes. Inhibition curves for the displacement of [^{3}H]CHIBA-1001 (30 nM) binding to rat brain cortex membranes by (±)-epibatidine, DMAB, A-58294, MG624, A-844606, SSR180711, PNU-282987, (–)-nicotine, α-bungarotoxin, and MLA. The K_i denotes the affinity constant for binding to a single state of binding sites. The results are means ± S.E.M. of three separate experiments performed in duplicate.

Table 1 – Drug inhibition of [^{3}H]CHIBA-1001 binding to rat brain membranes.

Drugs	Ki (nM)
SSR180711	31.4
A844606	827
MG624	1625
Epibatidine	2195
DMAB	2506
PNU-282987	3529
A582941	5161
α-Bungarotoxin	>100,000
MLA	>100,000
Nicotine	>100,000

The inhibition of [^{3}H]CHIBA-1001 binding by various drugs was determined with [^{3}H]CHIBA-1001 (30 nM). Nine concentrations of the drugs were used for each determination. Ki values for the various drugs were determined as described in Materials and methods. The values represent the mean of three determinations done in duplicate.

distribution of [^{125}I]α-bungarotoxin binding in the monkey brain was not similar to that of [^{3}H]CHIBA-1001 binding (Figs. 5 and 6). The differences in binding between [^{3}H]CHIBA-1001 and [^{125}I]α-bungarotoxin were seen in the thalamus and striatum, both of which were found to have fewer binding sites of [^{125}I]α-bungarotoxin (Fig. 6).

2.6. *Regional distribution of [^{3}H]CHIBA-1001 binding in the human brain*

The regional distributions of [^{3}H]CHIBA-1001 binding and [^{125}I]α-bungarotoxin binding in the postmortem brain samples from 2 human subjects are shown in Fig. 7. The regional distribution of [^{3}H]CHIBA-1001 binding was homogenous (Fig. 7A), while low binding of [^{125}I]α-bungarotoxin was detected in the thalamus, cerebellum, and pons (Fig. 7B).

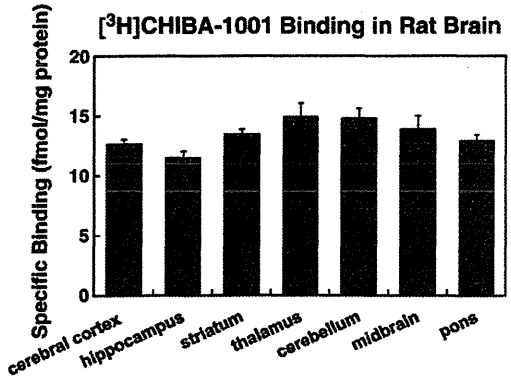

Fig. 4 – The regional distribution of [^{3}H]CHIBA-1001 binding in rat brain. Rat brains were dissected into seven regions, as described in Materials and methods. The regional distribution of [^{3}H]CHIBA-1001 (30 nM) binding in the rat brain was determined. The results are means ± S.E.M. of three separate experiments performed in duplicate.

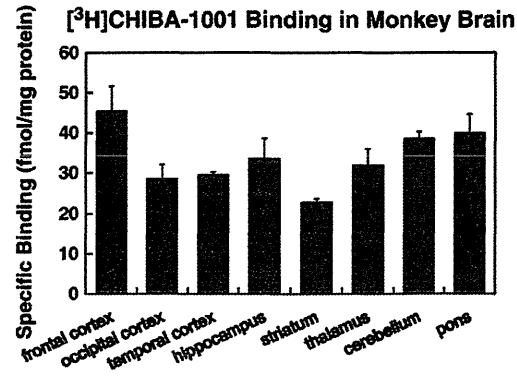

Fig. 5 – The regional distribution of [^{3}H]CHIBA-1001 binding in monkey brain. Monkey brains were dissected into eight regions, and the regional distribution of [^{3}H]CHIBA-1001 (30 nM) binding in the monkey brains was measured. The regional distribution of [^{3}H]CHIBA-1001 binding in the monkey brain was homogenous. The results are means ± S.E.M. of three separate experiments performed in duplicate.

3. Discussion

The present study suggests that [^{3}H]CHIBA-1001 would be a useful radioligand for labeling α7 nAChRs in brain membranes from rat, monkey, and human. We have previously reported that CHIBA-1001 (1 μM) is devoid of activity (inhibition lower than 50%) for a 28 standard receptor binding profiles, suggesting a high selectivity at α7 nAChRs (Hashimoto et al., 2008b). The saturation binding data of the present study indicate that [^{3}H]CHIBA-1001 binds with an affinity (Kd=193.4 nM) to an apparently homogeneous population of receptors (Bmax=346.2 fmol/mg protein) of rat cortex.

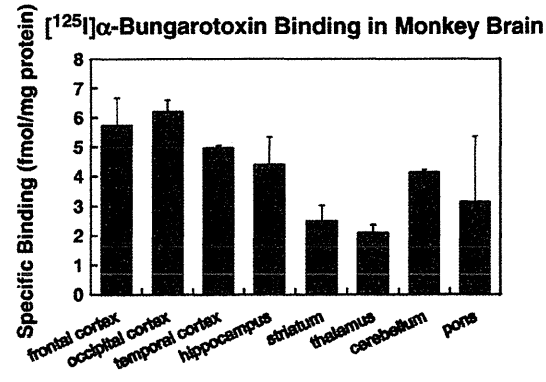

Fig. 6 – The regional distribution of [^{125}I]α-bungarotoxin binding in monkey brain. Monkey brains (n=2) were dissected into eight regions, and the binding of [^{125}I]α-bungarotoxin (0.8 nM) was measured in each region performed in duplicate in the same way as [^{3}H]CHIBA-1001. Unlike [^{3}H]CHIBA-1001, the radioactivity of [^{125}I]α-bungarotoxin binding was in the order of (highest to lowest) thalamus > midbrain > hippocampus > frontal cortex > pons > striatum > cerebellum.

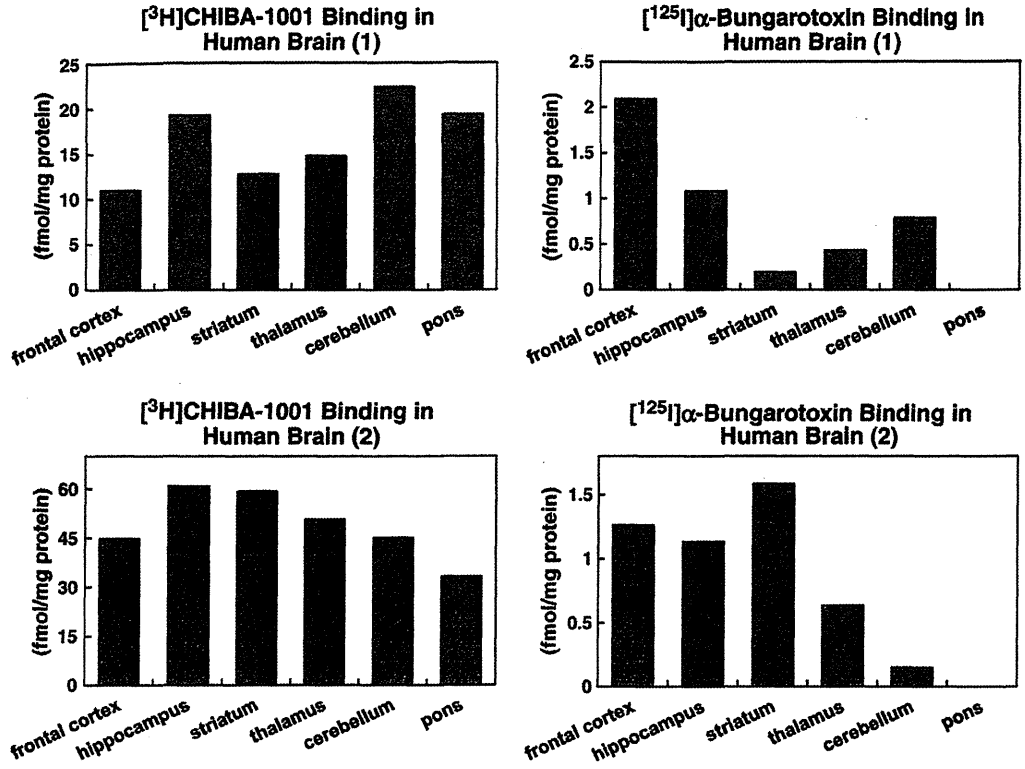

Fig. 7 – The regional distribution of [^{3}H]CHIBA-1001 binding and [^{125}I]α-bungarotoxin binding in the human brain. The regional distribution of [^{3}H]CHIBA-1001 (30 nM)(A) and [^{125}I]α-bungarotoxin (0.8 nM)(B) binding in the postmortem brain samples from 2 human subjects was measured. The regional distribution of [^{3}H]CHIBA-1001 binding was homogenous, whereas the distribution of [^{125}I]α-bungarotoxin binding was low in the cerebellum and pons. The results are the mean of data performed in duplicate.

The pharmacological inhibition study revealed some important points. Although the Ki values for the displacement of [^{3}H]CHIBA-1001 by a number of nAChR ligands were slightly higher than those obtained for other α7 nAChR ligands, as reported previously (Davies et al., 1999; Anderson et al., 2008), it is likely that the pharmacological specificity of [^{3}H]CHIBA-1001 could be related to α7 nAChRs because it was certainly inhibited by a number of α7 nAChRs ligands. In contrast, [^{3}H] CHIBA-1001 binding was not displaced by α-bungarotoxin and MLA, although [^{125}I]α-bungarotoxin binding was displaced by MLA as well as by SSR180711 and A-844606. It has been reported that Ki values for the displacement of [^{3}H]MLA binding by various α7 nAChR ligands correlate with those obtained in parallel for the displacement of [^{125}I]α-bungarotoxin binding (Davies et al., 1999), suggesting a similar pharmacology of these two radioligands. A recent study demonstrated that specific binding of [^{3}H]MLA to human frontal cortical membranes is not detectable due to high nonspecific binding levels, and that MLA shows considerably lower affinity at a new α7 nAChR radioligand, [^{3}H]A-585539, binding to human cortical membranes (Anderson et al., 2008), indicating a species difference (rat vs. human) for MLA's pharmacology. The reasons underlying the din of α-bungarotoxin or MLA inhibition on the [^{3}H]CHIBA-1001 binding and [^{125}I]α-bungarotoxin binding are currently unknown. It is unlikely that [^{3}H]CHIBA-1001 binding sites are identical to [^{125}I]α-bungarotoxin binding sites because α-bungarotoxin and MLA have high-molecular weight compounds as compared with the small size of α7 nAChR ligands such as SSR180711 and A-844606. It therefore seems that the [^{3}H] CHIBA-1001 binding characteristics may be different from those of [^{125}I]α-bungarotoxin binding in the brain although a further detailed study is necessary.

The α7 subunit of nAChRs is widely expressed in the brain, especially in regions associated with cognitive processing. In this study, we found that the regional distribution of [^{3}H]CHIBA-1001 binding was different from that of [^{125}I]α-bungarotoxin in the rat, monkey, and human brain. Our results show that high densities of α7 nAChRs can be found in the hippocampus, hypothalamus, and cortical areas in the rat brain. In this study, the high densities of [^{3}H]CHIBA-1001 binding sites in the hippocampus, thalamus, frontal cortex, and pons were similar to those of [^{125}I]α-bungarotoxin binding in the rat brain (Séguéla et al., 1993). The regional difference between these two ligands occurred in the cerebellum, where [^{3}H]CHIBA-1001 binding was high whereas [^{125}I]α-bungarotoxin binding was almost nonexistent. In adult rat cerebellum, α7 nAChRs were expressed in significant amounts, especially in the Purkinje cell layer P8–P15; they also appeared to play an important role in regulating calcium-dependent events, ultimately leading to developmental plasticity (Domínguez del Toro et al., 1997). It has been reported that a moderate density of α7 mRNA is present in

monkey and human cerebellum (Quik et al., 2000; Graham et al., 2002). The regional distribution of [^{3}H]CHIBA-1001 binding in the monkey brain seemed to be similar to the pattern in rat brain. It has been suggested that the distribution of [^{125}I]α-bungarotoxin binding is larger in the brains of rhesus monkeys than in rodent brain (Han et al., 2003). The reasons underlying the differences in the regional distribution of the [^{3}H]CHIBA-1001 binding and [^{125}I]α-bungarotoxin binding are currently unknown. The difference of molecular weight of two radioligands [^{3}H]CHIBA-1001 and [^{125}I]α-bungarotoxin may contribute to the regional differences in the brain although a further detailed study is needed.

In monkey brain, the region that appeared to make a difference in the binding of the two ligands was the thalamus, where [^{3}H]CHIBA-1001 binding was seen, as in other regions, while there was little [^{125}I]α-bungarotoxin binding. It has been reported that α7 nAChR mRNA is expressed in the thalamus, based on the use of *in situ* hybridization (Quik et al., 2000). Although the distribution of α7 nAChRs in primates is still not completely known, it has been suggested that the distribution of α7 nAChRs in the monkey brain is more similar to that in humans than in rodents (Quik et al., 2000). This difference between rodents and primates may reflect an increased need for thalamocortical modulation in the human neocortex (Breese et al., 1997), because activation of the α7 nAChRs by cholinergic afferents could modulate inhibitory activity and sensory processing within the corticothalamic axis. In this study, we found a regional difference in distribution between [^{3}H]CHIBA-1001 binding and [^{125}I]α-bungarotoxin binding in the human brain, although the reasons underlying this discrepancy are unknown.

Unlike [^{3}H]CHIBA-1001 binding, the density of [^{125}I]α-bungarotoxin binding was low in the cerebellum. In the human brain, α7 nAChRs have been shown to be distributed in regions related to cognitive function such as the nucleus accumbens, ventral hippocampus, amygdala, and frontal cortex (Levin et al., 2006; Nashmi and Lester, 2006). In addition, it has been suggested that the cerebellum is also involved in cognition, behavior, and emotion (Frings et al., 2007). For example, preliminary studies employing histoblots of cerebellar sections have suggested a higher concentration of α7 nAChR subunits in the molecular layer, and the immunohistochemistry in fixed tissue indicates that Purkinje cells strongly express α7 subunits (Court et al., 2000). Another report has reported the observation of α7 nAChRs mRNA and protein in various cells in the cerebellum (Graham et al., 2002; Hellström-Lindahl et al., 1998). For labeling α7 nAChRs in the cerebellum, it seems that [^{3}H]CHIBA-1001 may have a distinct advantage over [^{125}I]α-bungarotoxin. Thus, it is likely that [^{3}H]CHIBA-1001 could be a suitable radioligand for labeling α7 nAChRs in the cerebellum, although further study will be necessary.

The new radioligand [^{3}H]CHIBA-1001 may, however, have some limitations to its use. One is the relatively low affinity (Kd = 193.4 nM) of [^{3}H]CHIBA-1001 binding to crude brain membranes, suggesting that the practicality of this radioligand may be limited. Alternatively, a new radioligand, [^{3}H]A-585539, has demonstrated high-affinity binding consistent with α7 nAChRs pharmacology, a rapid association rate, and a relatively slow dissociation rate (Anderson et al., 2008). Another limitation is the high proportion (approximately 50%) of nonspecific binding of [^{3}H]CHIBA-1001 in the brain membranes, whereas nonspecific binding of [^{3}H]A-585539 has been found to be less than 10% of total binding (Anderson et al., 2008). As such, [^{3}H]A-585539 may be better than [^{3}H]CHIBA-1001 for labeling α7 nAChRs in the brain, although a further detailed study is necessary.

In conclusion, the present study suggests that [^{3}H]CHIBA-1001 would be a suitable radioligand for the *in vitro* labeling of α7 nAChRs in the brain. It is therefore likely that [^{3}H]CHIBA-1001 could be a useful radioligand for studying α7 nAChRs in postmortem brain samples from patients with neuropsychiatric diseases such as schizophrenia and Alzheimer's disease.

4. Experimental procedures

4.1. *Synthesis of [^{3}H]CHIBA-1001*

CHIBA-1001 and its precursor, 4-(tributylstannyl)phenyl 2,5-diazabicyclo[3.2.2]nonane -2-carboxylate (Fig. 1), were synthesized as described previously (Hashimoto et al., 2008b).

[^{3}H]CHIBA-1001 was synthesized by *N*-methylation of the precursor with [^{3}H]methyl iodide (Fig. 1). A 0.1-mL quantity of [^{3}H]methyl iodide toluene solution (370 MBq) (American Radiolabeled Chemicals, Inc., St. Louis, MO) was added to the ice-cold reaction vessel, which contained tris(dibenzylideneaceton) dipalladium (2.8 mg), tri-o-tolylphosphine (3.7 mg), the precursor (0.8 mg), copper (I) chloride (1.2 mg), and potassium carbonate (1.7 mg) in *N*,*N*-dimethylformamide DMF (0.3 ml). The reaction vessel was heated at 80 °C for 5 min. The mixture of reaction solution was transferred to the high-performance liquid chromatography (HPLC) injection unit through a glass filter to remove solid reagents, and injected into a preparative HPLC system using an YMC-Pack Pro C18 column (10 mm in inner diameter × 250 mm in length, YMC Co., Ltd., Kyoto, Japan). The radioactive peak fraction eluted by CH_3CN/50 mM CH_3COONH_4/CH_3COOH (250/750/3) at a flow rate of 4 ml/min was collected into an evaporation flask and evaporated; the residue was then re-dissolved with 2 ml of ethanol.

Chemical and radiochemical analyses of [^{3}H]CHIBA-1001 were performed by HPLC in a system consisting of a column (YMC-Pack Pro C18, 4.6 mm in inner diameter × 250 mm in length, YMC Co., Ltd., Kyoto, Japan) and the use of CH_3CN/50 mM CH_3COONH_4/CH_3COOH (250/750/3) as a mobile phase at a flow rate of 1 ml/min.

4.2. *Membrane preparation*

[^{3}H]CHIBA-1001 (2960 GBq/mmol) binding was performed using membrane-enriched fractions from rat, monkey, and human brain. For most of the experiments, male Crl:CD(SD) SPF/VAF rats (180–200 g) (Japan Charles River Inc., Tokyo, Japan) were used. The rats were killed by decapitation, and the brains were rapidly removed. The brains were dissected on ice into 7 sections, the frontal cortex, hippocampus, thalamus, striatum, cerebellum, midbrain, and pons (including medulla oblongata), by the method of Glowinski and Iversen (1966) and then stored at −80 °C until use. The brain was homogenized in 15 volumes of 0.32 M sucrose using a Teflon glass homogenizer and centrifuged at 1000 × *g* for 10 min (4 °C). The

supernatant was centrifuged at 48,000×*g* for 20 min (4 °C). The resultant pellets were homogenized in the buffer (120 mM NaCl, 5 mM KCl, 2 mM $CaCl_2$, 2 mM $MgCl_2$, 50 mM Tris–HCl, pH 7.4 at 4 °C) with a Polytron and spun at 48,000×*g* for 20 min (4 °C). The membrane pellets were washed and re-suspended in ice-cold buffer and were then centrifuged two more times before storage at −80 °C. The final pellet was re-suspended in 10 volumes of the same buffer. Protein concentrations were measured according to the method of Lowry et al. (1951).

Brain samples of three male *Macaca fascicularis* (4560 g, 4890 g, and 4680 g) were provided by Hamamatsu photonics (Hamamatsu, Japan). The brains were dissected on ice into 8 sections, the frontal cortex, occipital cortex, temporal cortex, hippocampus, thalamus, striatum, cerebellum, and pons (including medulla oblongata), and then stored at −80 °C until use.

Postmortem human brain samples (n=2; one is male, age 77, Caucasian, liver cancer as cause of death, smoked 2–3 packs of cigarettes per day for 37 years — quit 24 years prior to death; the other is male, age 77, Caucasian, pulmonary fibrosis as cause of death, smoked 1 pack of cigarettes per day for 25 years — quit 5 years prior to death) were purchased from Analytical Biological Service Inc. (Cornell Business Park, Wilmington, DE) in the form of frozen 2–3 g blocks of each of 6 sections, the frontal cortex, hippocampus, thalamus, striatum, cerebellum, and pons. These samples were stored at −80 °C until use. The brain was further dissected on ice into 0.2–0.3 g for the binding assay, and membrane preparation was conducted in the same way as for rat brain, except for the process of homogenizing in 15 volumes of 0.32 M sucrose using a Teflon glass homogenizer and centrifugation at 1000×*g* for 10 min (4 °C); the pellet was then discarded.

The experimental procedures using rats, monkeys, and human postmortem brain samples were approved by the Animal Care and Use Committee and Ethics Committee of Chiba University.

4.3. [^{3}H]CHIBA-1001 binding assay

Aliquots of membrane suspension (200 μl) were added, in duplicate, to the reaction mixture containing [^{3}H]CHIBA-1001 and the indicated concentrations of test drug in a final volume of 0.5 ml. Nonspecific binding was estimated in the presence of 50 μM SSR180711. Binding was allowed to occur for 150 min at 4 °C. Bound radioactivity was isolated by rapid vacuum filtration onto Whatman GF/B glass filters pretreated with 0.5% polyethyleneimine (Sigma-Aldrich Corporation, St. Louis, MO) for 3–4 h using a 24-channel cell harvester (Brandell, Gaithersburg, MD). The filters were washed with 5 ml of ice-cold buffer 3 times. The radioactivity trapped by the filters was determined using a liquid scintillation counter (Beckman, LS-6500, Beckman Coulter K.K., Tokyo, Japan).

To examine the pharmacological profiles of [^{3}H]CHIBA-1001 binding, ten kinds of α7 nAChR compounds, including PNU-282987, MG624, (±)-epibatidine, MLA, α-bungarotokin, (−)-nicotine (Sigma-Aldrich, St. Louis, MO), DMAB-anabaseine dihydrochloride (Tocris, Bristol, UK), A-582941, A-844606, and SSR180711 (synthesized in our laboratory) were used.

Regional distribution of [^{3}H]CHIBA-1001 binding of each brain was compared to that of [^{125}I]α-bungarotoxin (5.92 TBq/mmol, PerkinElmer Life Sciences, Inc., Boston, MA) binding. The binding assay of [^{125}I]α-bungarotoxin was performed in the same way of the [^{3}H]CHIBA-1001 binding assay, except for the incubation condition (180 min at 37 °C) and filter pretreatment (0.5% polyethyleneimine with 0.1% bovine serum albumin).

4.4. Data analysis

The data show the mean±standard error of the mean (S.E.M.). Dissociation constant (Kd) and maximal binding (Bmax) values from saturation binding and IC_{50} values from binding displacement by some drugs were determined using GraphPad Prism (GraphPad Software, San Diego, CA). Ki values were calculated from the IC_{50} values using Microsoft Excel, where $Ki = IC_{50}/(1+[Ligand]/Kd)$(Cheng and Prusoff, 1973).

Acknowledgments

This work was supported by grant from the Program for Promotion of Fundamental Studies in Health Sciences of the National Institute of Biomedical Innovation of Japan (grant ID: 06-46, to K.H.).

Appendix A. Supplementary data

Supplementary data associated with this article can be found, in the online version, at doi:10.1016/j.brainres.2010.06.008.

REFERENCES

Adams, C.E., Stevens, K.E., 2007. Evidence for a role of nicotinic acetylcholine receptors in schizophrenia. Front. Biosci. 12, 4755–4772.

Anderson, D.J., Bunnelle, W., Surber, B., Du, J., Surowy, C., Tribollet, E., Marguerat, A., Bertrand, D., Gopalakrishnan, M., 2008. [3H]A-585539 [(1 S, 4 S)-2, 2-dimethyl-5-(6-phenylpyridazin-3-yl)-5-aza-2-azoniabicyclo [2.2.1]heptane], a novel high-affinity α7 neuronal nicotinic receptor agonist: radioligand binding characterization to rat and human brain. J. Pharmacol. Exp. Ther. 324, 179–187.

Barak, S., Arad, M., De Levie, A., Black, M.D., Griebel, G., Weiner, I., 2009. Pro-cognitive and antipsychotic efficacy of the α7 nicotinic partial agonist SSR180711 in pharmacological and neurodevelopmental latent inhibition models of schizophrenia. Neuropsychopharmacology 34, 1753–1763.

Bitner, R.S., Bunnelle, W.H., Anderson, D.J., Briggs, C.A., Buccafusco, J., Curzon, P., Decker, M.W., Frost, J.M., Gronlien, J.H., Gubbins, E., Li, J., Malysz, J., Markosyan, S., Marsh, K., Meyer, M.D., Nikkel, A.L., Radek, R.J., Robb, H.M., Timmermann, D., Sullivan, J.P., Gopalakrishnan, M., 2007. Broad-spectrum efficacy across cognitive domains by α7 nicotinic acetylcholine receptor agonism correlates with activation of ERK1/2 and CREB phosphorylation pathways. J. Neurosci. 27, 10578–10587.

Biton, B., Bergis, O.E., Galli, F., Nedelec, A., Lochead, A.W., Jegham, S., Godet, D., Lanneau, C., Santamaria, R., Chesney, F., Léonardon, J., Granger, P., Debono, M.W., Bohme, G.A., Sgard, F., Besnard, F., Graham, D., Coste, A., Oblin, A., Curet, O., Vigé, X., Voltz, C., Rouquier, L., Souilhac, J., Santucci, V., Gueudet, C.,

Françon, D., Steinberg, R., Griebel, G., Oury-Donat, F., George, P., Avenet, P., Scatton, B., 2007. SSR180711, a novel selective α7 nicotinic receptor partial agonist: (1) binding and functional profile. Neuropsychopharmacology 32, 1–16.

Bodnar, A.L., Cortes-Burgos, L.A., Cook, K.K., Dinh, D.M., Groppi, V.E., Hajos, M., Higdon, N.R., Hoffmann, W.E., Hurst, R.S., Myers, J.K., Rogers, B.N., Wall, T.M., Wolfe, M.L., Wong, E., 2005. Discovery and structure–activity relationship of quinuclidine benzamides as agonists of α7 nicotinic acetylcholine receptors. J. Med. Chem. 48, 905–908.

Breese, C.R., Adams, C., Logel, J., Drebing, C., Rollins, Y., Barnhart, M., Sullivan, B., Demasters, B.K., Freedman, R., Leonard, S., 1997. Comparison of the regional expression of nicotinic acetylcholine receptor α7 mRNA and [^{125}I]-α-bungarotoxin binding in human postmortem brain. J. Comp. Neurol. 387, 385–398.

Burghaus, L., Schütz, U., Krempel, U., de Vos, R.A., Jansen Steur, E.N., Wevers, A., Lindstrom, J., Schröder, H., 2000. Quantitative assessment of nicotinic acetylcholine receptor proteins in the cerebral cortex of Alzheimer patients. Brain Res. Mol. Brain Res. 76, 385–388.

Cheng, Y.C., Prusoff, W.H., 1973. Relathionship between the inhibition constant (Ki) and concentration of inhibitor which causes 50 percent inhibition (IC_{50}) of an enzymatic reaction. Biochem. Pharmacol. 22, 3099–3108.

Court, J.A., Martin-Ruiz, C., Graham, A., Perry, E., 2000. Nicotinic receptors in human brain: topography and pathology. J. Chem. Neuroanat. 20, 281–298.

Court, J.A., Martin-Ruiz, C., Piggott, M., Spurden, D., Griffiths, M., Perry, E., 2001. Nicotinic receptor abnormalities in Alzheimer's disease. Biol. Psychiatry 49, 175–184.

Davies, A.R., Hardick, D.J., Blagbrough, I.S., Potter, B.V., Wolstenholme, A.J., Wonnacott, S., 1999. Characterisation of the binding of [^{3}H] methyllycaconitine: a new radioligand for labelling α7-type neuronal nicotinic acetylcholine receptors. Neuropharmacology 38, 679–690.

Deuther-Conrad, W., Fischer, S., Hiller, A., Nielsen, E.Ø., Timmermann, D.B., Steinbach, J., Sabri, O., Peters, D., Brust, P., 2009. Molecular imaging of α7 nicotinic acetylcholine receptors: design and evaluation of the potent radioligand [^{18}F] NS10743. Eur. J. Nucl. Med. Mol. Imaging 36, 791–800.

Domínguez del Toro, E., Juíz, J.M., Smillie, F.I., Lindstrom, J., Criado, M., 1997. Expression of α7 neuronal nicotinic receptors during postnatal development of the rate cerebellum. Brain Res. Dev. Brain Res. 98, 125–133.

Dziewczapolski, G., Glogowski, C.M., Masliah, E., Heinemann, S.F., 2009. Deletion of the α7 nicotinic acetylcholine receptor gene improves cognitive deficits and synaptic pathology in a mouse model of Alzheimer's disease. J. Neurosci. 29, 8805–8815.

Freedman, R., Hall, M., Adler, L.E., Leonard, S., 1995. Evidence in postmortem brain tissue for decreased numbers of hippocampal nicotinic receptors in schizophrenia. Biol. Psychiatry 38, 22–33.

Frings, M., Maschke, M., Timmann, D., 2007. Cerebellum and cognition — viewed from philosophy of mind. Cerebellum 12, 1–7.

Glowinski, J., Iversen, L.L., 1966. Regional studies of catecholamines in the rat brain. I. The disposition of [^{3}H] norepinephrine, [^{3}H]dopamine and [^{3}H]dopa in various regions of the brain. J. Neurochem. 13, 655–669.

Graham, A., Court, J.A., Martin-Ruiz, C.M., Jaros, E., Perry, R., Volsen, S.G., Bose, S., Evans, N., Ince, P., Kuryatov, A., Lindstrom, J., Gotti, C., Perry, E.K., 2002. Immunohistochemical localisation of nicotinic acetylcholine receptor subunits in human cerebellum. Neuroscience 113, 493–507.

Hajós, M., Hurst, R.S., Hoffmann, W.E., Krause, M., Wall, T.M., Higdon, N.R., Groppi, V.E., 2005. The selective α7 nicotinic acetylcholine receptor agonist PNU-282987 [N-[(3R)-1-Azabicyclo [2.2.2]oct-3-yl]-4-chlorobenzamide hydrochloride] enhances GABAergic synaptic activity in brain slices and restores auditory gating deficits in anesthetized rats. J. Pharmacol. Exp. Ther. 312, 1213–1222.

Han, Z.Y., Zoli, M., Cardona, A., Bourgeois, J.P., Changeux, J.P., Le Novère, N., 2003. Localization of [^{3}H]nicotine, [^{3}H]cytisine, [^{3}H] epibatidine, and [^{125}I]α-bungarotoxin binding sites in the brain of Macaca mulatta. J. Comp. Neurol. 461, 49–60.

Hashimoto, K., Iyo, M., 2002. Amyloid cascade hypothesis of Alzheimer's disease and α7 nicotinic receptor. Nihon Shinkei Seishin Yakurigaku Zasshi 22, 49–53.

Hashimoto, K., Koike, K., Shimizu, E., Iyo, M., 2005. α7 Nicotinic receptor agonists as potential therapeutic drugs for schizophrenia. Curr. Med. Chem.-CNS Agents 5, 171–184.

Hashimoto, K., Fujita, Y., Ishima, T., Hagiwara, H., Iyo, M., 2006. Phencyclidine-induced cognitive deficits in mice are improved by subsequent subchronic administration of tropisetron: role of α7 nicotinic receptors. Eur. J. Pharmacol. 553, 191–195.

Hashimoto, K., Ishima, T., Fujita, Y., Matsuo, M., Kobashi, T., Takahagi, M., Tsukada, H., Iyo, M., 2008a. Phencyclidine-induced cognitive deficits in mice are improved by subsequent subchronic administration of the novel selective α7 nicotinic receptor agonist SSR180711. Biol. Psychiatry 63, 92–97.

Hashimoto, K., Nishiyama, S., Ohba, H., Matsuo, M., Kobashi, T., Takahagi, M., Iyo, M., Kitashoji, T., Tsukada, H., 2008b. [^{11}C] CHIBA-1001 as a novel PET ligand for α7 nicotinic receptors in the brain: a PET study in conscious monkeys. PLoS ONE 3, e3231.

Hellström-Lindahl, E., Gorbounova, O., Seiger, A., Mousavi, M., Nordberg, A., 1998. Regional distribution of nicotinic receptors during prenatal development of human brain and spinal cord. Brain Res. Dev. Brain Res. 108, 147–160.

Hellström-Lindahl, E., Mousavi, M., Zhang, X., Ravid, R., Nordberg, A., 1999. Regional distribution of nicotinic receptor subunit mRNAs in human brain: comparison between Alzheimer and normal brain. Brain Res. Mol. Brain Res. 66, 94–103.

Kim, S.W., Ding, Y.S., Alexoff, D., Patel, V., Logan, J., Lin, K.S., Shea, C., Muench, L., Xu, Y., Carter, P., King, P., Constanzo, J.R., Ciaccio, J.A., Fowler, J.S., 2007. Synthesis and positron emission tomography studies of C-11-labeled isotopomers and metabolites of GTS-21, a partial α7 nicotinic cholinergic agonist drug. Nucl. Med. Biol. 34, 541–551.

Levin, E.D., Bettegowda, C., Blosser, J., Gordon, J., 1999. AR-R17779, and α7 nicotinic agonist, improves learning and memory in rats. Behav. Pharmacol. 10, 675–680.

Levin, E.D., McClernon, F.J., Rezvani, A.H., 2006. Nicotinic effects on cognitive function: behavioral characterization, pharmacological specification, and anatomic localization. Psychopharmacology (Berl) 184, 523–539.

Lowry, O.H., Rosebrough, N.J., Farr, A.L., Randall, R.J., 1951. Protein measurement with the Folin phenol reagent. J. Biol. Chem. 193, 265–275.

Martin, L.F., Kem, W.R., Freedman, R., 2004. α7 nicotinic receptor agonists: potential new candidates for the treatment of schizophrenia. Psychopharmacology (Berl) 174, 54–64.

Marutle, A., Zhang, X., Court, J., Piggott, M., Johnson, M., Perry, R., Perry, E., Nordberg, A., 2001. Laminar distribution of nicotinic receptor subtypes in cortical regions in schizophrenia. J. Chem. Neuroanat. 22, 115–126.

Nashmi, R., Lester, H.A., 2006. CNS localization of neuronal nicotinic receptors. J. Mol. Neurosci. 30, 181–184.

Ogawa, M., Tatsumi, R., Fujio, M., Katayama, J., Magata, Y., 2006. Synthesis and evaluation of [^{125}I]I-TSA as a brain nicotinic acetylcholine receptor α7 subtype imaging agent. Nucl. Med. Biol. 33, 311–316.

Ogawa, M., Tsukada, H., Hatano, K., Ouchi, Y., Saji, H., Magata, Y., 2009. Central *in vivo* nicotinic acetylcholine receptor imaging agents for positron emission tomography (PET) and single